Transition form factors and angular distributions of the $\Lambda_b \to \Lambda(1520)(\to N\bar{K})\ell^+\ell^-$ decay supported by baryon spectroscopy

Yu-Shuai Li,[1,2,*] Su-Ping Jin,[3,†] Jing Gao,[3,‡] and Xiang Liu[1,2,4,5,§]

[1]School of Physical Science and Technology, Lanzhou University, Lanzhou 730000, China
[2]Research Center for Hadron and CSR Physics, Lanzhou University and Institute of Modern Physics of CAS, Lanzhou 730000, China
[3]School of Physics, Nankai University, Tianjin 300071, China
[4]Lanzhou Center for Theoretical Physics, Key Laboratory of Theoretical Physics of Gansu Province, and Frontiers Science Center for Rare Isotopes, Lanzhou University, Lanzhou 730000, China
[5]Key Laboratory of Quantum Theory and Applications of MoE, Lanzhou University, Lanzhou 730000, China

(Received 11 October 2022; accepted 19 April 2023; published 11 May 2023)

We calculate the weak transition form factors of the $\Lambda_b \to \Lambda(1520)$ transition, and further calculate the angular distributions of the rare decays $\Lambda_b \to \Lambda(1520)(\to N\bar{K})\ell^+\ell^-$ ($N\bar{K} = \{pK^-, n\bar{K}^0\}$) with unpolarized Λ_b and massive leptons. The form factors are calculated by the three-body light-front quark model with the support of numerical wave functions of Λ_b and $\Lambda(1520)$ from solving the semirelativistic potential model associated with the Gaussian expansion method. By fitting the mass spectrum of the observed single bottom and charmed baryons, the parameters of the potential model are fixed, so this strategy can avoid the uncertainties arising from the choice of a simple harmonic oscillator wave function of the baryons. With more data accumulated in the LHCb experiment, our result can help for exploring the $\Lambda_b \to \Lambda(1520)\ell^+\ell^-$ decay and deepen our understanding on the $b \to s\ell^+\ell^-$ processes.

DOI: 10.1103/PhysRevD.107.093003

I. INTRODUCTION

The flavor-changing neutral-current (FCNC) processes, including the high-profile $b \to s\ell^+\ell^-$ process, can play a crucial role in indirect searches for physics beyond the Standard Model (SM). These transitions are forbidden at the tree level and can only operate through loop diagrams in the SM, and are therefore highly sensitive to potential new physics (NP) effects, such as the much-discussed $R_{D^{(*)}} = \mathcal{B}(B \to D^{(*)}\tau\nu_\tau)/\mathcal{B}(B \to D^{(*)}e(\mu)\nu_{e(\mu)})$ [1–4]. These processes thus provided a unique platform to deepen our understanding of both quantum chromodynamics (QCD) and the dynamics of weak processes, and to help hunt for NP signs. Therefore, the rare decays of $b \to s$ have attracted the attention of both theorists and experimentalists [5–11].

For example, the rare decay $\Lambda_b \to \Lambda\ell^+\ell^-$ has been theoretically studied by various approaches, including lattice QCD (LQCD) [12,13], QCD sum rules [14], light-cone sum rule [15–19], covariant quark model [20], nonrelativistic quark model (NRQM) [21,22], and the Bethe-Salpeter approach [23], etc., and was first measured by the CDF Collaboration [7] and later by the LHCb Collaboration [8,9]. In addition to the differential branching ratio, such abundant phenomenologies of various angular distributions have also been studied. Compared with the measured data, the angular distribution of $\Lambda_b \to \Lambda\ell^+\ell^-$ was studied in Refs. [24,25] with unpolarized Λ_b baryon, and with polarized Λ_b baryon in Ref. [26]. Furthermore, the authors studied the $b \to s\mu^+\mu^-$ Wilson coefficients in Ref. [27] using the measured full angular distribution of the rare decay $\Lambda_b \to \Lambda(\to p\pi)\mu^+\mu^-$ by the LHCb Collaboration [9].

With the previous experiences on the decay to the ground state Λ, it is therefore worth further testing the $b \to s\ell^+\ell^-$ transition in the baryon sector decaying to the excited hyperon with quantum number being $J^P = 3/2^-$. The form factors of the weak transition were calculated by the quark model [21,22], LQCD [28,29]. and the heavy quark expansion [30]. The angular analysis was performed in Ref. [31] and Ref. [32] for massless and massive leptons, respectively. The authors of Ref. [33] studied the kinematic endpoint relations for $\Lambda_b \to \Lambda(1520)\ell^+\ell^-$ decays and

*liysh20@lzu.edu.cn
†jinsuping@nankai.edu.cn
‡9820210055@nankai.edu.cn
§xiangliu@lzu.edu.cn

provided the corresponding angular distributions. Amhis *et al.* [34] used the dispersive techniques to provide a model-independent parametrization of the form factors of $\Lambda_b \to \Lambda(1520)$ and further investigated the FCNC decay $\Lambda_b \to \Lambda(1520)\ell^+\ell^-$ with the LQCD data. In addition, Xing *et al.* also studied the multibody decay $\Lambda_b \to \Lambda_J^*(\to pK^-)J/\psi(\to \ell^+\ell^-)$ [35]. In addition, Amhis *et al.* studied the angular distributions of $\Lambda_b \to \Lambda(1520)\ell^+\ell^-$ and talked about the potential to identify NP effects [36]. Obviously, the $\Lambda_b \to \Lambda(1520)$ is less studied. Following this line, we further study the $\Lambda_b \to \Lambda(1520)(\to N\bar{K})\ell^+\ell^-$ with the $N\bar{K} = \{pK^-, n\bar{K}^0\}$ process and investigate the corresponding angular observables.

From a theoretical point of view, apart from the consideration of new operators beyond the SM, the calculation of the weak transition form factors is a key issue. In addition, how to solve the three-body system for the Λ_b baryon and Λ^* hyperon involved is also a challenge. In previous work on baryon weak decays [37–41], the quark-diquark scheme has been widely adopted as an approximate treatment. Meanwhile, the spatial wave functions of hadrons are often approximated as simple harmonic oscillator (SHO) wave functions [37–43], which makes the results dependent on the relevant parameters. To avoid the correlative uncertainties of the above approximations, in this work we calculate the $\Lambda_b \to \Lambda^*$ form factors by the three-body light-front quark model. Moreover, in the realistic calculation, we take the numerical spatial wave functions as input, where the semirelativistic potential model combined with the Gaussian expansion method (GEM) [44–47] is adopted. By fitting the mass spectrum of the observed single bottom and charmed baryons, the parameters of the semirelativistic potential model can be fixed. Compared with the SHO wave function approximation, our strategy can avoid the uncertainties arising from the selection of the spatial wave functions of the baryons.

The structure of this paper is as follows. After the Introduction, we derive the helicity amplitudes of $\Lambda_b \to \Lambda^*(\to N\bar{K})\ell^+\ell^-$ $(N\bar{K} = \{pK^-, n\bar{K}^0\})$ processes and define some angular observables with unpolarized Λ_b baryons and massive leptons in Sec. II. The formulas for the weak transition form factors are derived in the three-body light-front quark model in Sec. III. And then, to obtain the spatial wave functions of the involved baryons, the applied semirelativistic potential model and GEM are briefly introduced in Sec. IV. In Sec. V, we present our numerical results, including both the relevant form factors and the physical observables in $\Lambda_b \to \Lambda^*(\to N\bar{K})\ell^+\ell^-$ decays. Finally, this paper ends with a short summary in Sec. VI.

II. THE ANGULAR DISTRIBUTION OF $\Lambda_b \to \Lambda^*(\to N\bar{K})\ell^+\ell^-$

In this paper, we use a model-independent approach with the effective Hamiltonian [48,49]

$$\mathcal{H}_{\rm eff}(b \to s\ell^+\ell^-) = -\frac{4G_F}{\sqrt{2}} V_{tb}V_{ts}^* \sum_{i=1}^{10} \mathcal{C}_i(\mu)\mathcal{O}_i(\mu) \quad (2.1)$$

to study the $b \to s\ell^+\ell^-$ process, where $G_F = 1.16637 \times 10^{-5}$ GeV^{-2} is the Fermi coupling constant and $|V_{tb}V_{ts}^*| = 0.04088$ [12] is the product of the Cabibbo-Kobayashi-Maskawa matrix elements. Furthermore, the Wilson coefficients $\mathcal{C}_i(\mu)$ describe the short-distance physics, while the four fermion operators $\mathcal{O}_i(\mu)$ describe the long-distance physics, where $\mathcal{O}_{1,2}$ are the current-current operators, $\mathcal{O}_{3-6}$ are the QCD penguin operators, $\mathcal{O}_{7,8}$ denote the electromagnetic and chromomagnetic penguin operators respectively, and $\mathcal{O}_{9,10}$ stand for the semileptonic operators.

In our calculation, we follow the treatment given in Refs. [6,23], adding the factorable quark-loop contributions from $\mathcal{O}_{1-6}$ and $\mathcal{O}_8$ to the effective Wilson coefficients $\mathcal{C}_7^{\rm eff}$ and $\mathcal{C}_9^{\rm eff}$. The effective Hamiltonian can be written as

$$\begin{aligned}\mathcal{H}_{\rm eff}(b \to s\ell^+\ell^-) = -\frac{4G_F}{\sqrt{2}} V_{tb}V_{ts}^* \frac{\alpha_e}{4\pi}\Big\{ &\bar{s}\Big[\mathcal{C}_9^{\rm eff}(\mu, q^2)\gamma^\mu P_L \\ &- \frac{2m_b}{q^2}\mathcal{C}_7^{\rm eff}(\mu) i\sigma^{\mu\nu}q_\nu P_R\Big] b(\bar{\ell}\gamma_\mu \ell) \\ &+ \mathcal{C}_{10}(\mu)(\bar{s}\gamma^\mu P_L b)(\bar{\ell}\gamma_\mu\gamma^5\ell)\Big\}, \quad (2.2)\end{aligned}$$

where $P_{R(L)} = (1 \pm \gamma^5)/2$ and $\sigma^{\mu\nu} = i[\gamma^\mu, \gamma^\nu]/2$. The electromagnetic coupling constant is $\alpha_e = 1/137$. For the leading logarithmic approximation, we take $m_b = 4.80$ GeV [50,51] and the Wilson coefficients as $\mathcal{C}_7^{\rm eff}(m_b) = -0.313$ and $\mathcal{C}_{10}(m_b) = -4.669$ in the calculation [50–53]. In addition, the short-distance contributions from the soft-gluon emission and the one-loop contributions of the four-quark operators $\mathcal{O}_1$-$\mathcal{O}_6$, and the long-distance effects due to the charmonium resonances, J/ψ and $\psi(2S)$ are taken into account, where we adopt the $\mathcal{C}_9^{\rm eff}(\mu, q^2)$ as [50,54,55]

$$\mathcal{C}_9^{\rm eff}(\mu, q^2) = \mathcal{C}_9(\mu) + Y_{\rm pert}(\hat{s}) + Y_{\rm res}(q^2). \quad (2.3)$$

The $Y_{\rm pert}$ term can be written as

$$\begin{aligned}Y_{\rm pert}(\hat{s}) = &\, g(\hat{m}_c, \hat{s})\mathcal{C}(\mu) \\ &- \frac{1}{2}g(1, \hat{s})(4\mathcal{C}_3(\mu) + 4\mathcal{C}_4(\mu) + 3\mathcal{C}_5(\mu) + \mathcal{C}_6(\mu)) \\ &- \frac{1}{2}g(0, \hat{s})(\mathcal{C}_3(\mu) + 3\mathcal{C}_4(\mu)) \\ &+ \frac{2}{9}(3\mathcal{C}_3(\mu) + \mathcal{C}_4(\mu) + 3\mathcal{C}_5(\mu) + \mathcal{C}_6(\mu)), \quad (2.4)\end{aligned}$$

where $\hat{m}_c = m_c/m_b$, $\hat{s} = q^2/m_b^2$, $\mathcal{C}(\mu) = 3\mathcal{C}_1(\mu) + \mathcal{C}_2(\mu) + 3\mathcal{C}_3(\mu) + \mathcal{C}_4(\mu) + 3\mathcal{C}_5(\mu) + \mathcal{C}_6(\mu)$, and [50]

$$g(z,\hat{s}) = -\frac{8}{9}\ln z + \frac{8}{27} + \frac{4}{9}x - \frac{2}{9}(2+x)\sqrt{|1-x|}\times\begin{cases}\ln\left|\frac{1+\sqrt{1-x}}{1-\sqrt{1-x}}\right| - i\pi & \text{for } x \equiv 4z^2/\hat{s} < 1\\ 2\arctan\frac{1}{\sqrt{x-1}} & \text{for } x \equiv 4z^2/\hat{s} > 1\end{cases},$$
$$g(0,\hat{s}) = \frac{8}{27} - \frac{8}{9}\ln\frac{m_b}{\mu} - \frac{4}{9}\ln\hat{s} + \frac{4}{9}i\pi. \tag{2.5}$$

The Wilson coefficients are used as $\mathcal{C}_1(m_b) = -0.248$, $\mathcal{C}_2(m_b) = 1.107$, $\mathcal{C}_3(m_b) = 0.011$, $\mathcal{C}_4(m_b) = -0.026$, $\mathcal{C}_5(m_b) = 0.007$, and $\mathcal{C}_6(m_b) = -0.031$ [50]. Besides, $m_c = 1.4$ GeV [50]. The $Y_{\rm res}$ term can be parametrized by using the Breit-Wigner ansatz (it is a model-dependent treatment, and one can refer to Refs. [56,57] for more detailed discussions) as [51]

$$Y_{\rm res}(q^2) = \frac{3\pi}{\alpha_e^2}C^{(0)}\sum_{V_i=J/\psi,\psi(2S)}\kappa_{Vi}\frac{\Gamma(V_i\to\ell^+\ell^-)m_{V_i}}{m_{V_i}^2 - q^2 - im_{V_i}\Gamma_{V_i}}, \tag{2.6}$$

where $C^{(0)} = 0.362$, $\kappa_{J/\psi} = 1$, and $\kappa_{\psi(2S)} = 2$. The masses and total widths associated with the relevant charmonium resonances are taken to be 3.096 GeV and 92.9 keV for J/ψ, and 3.686 GeV and 294 keV for $\psi(2S)$ [58]. The decay widths are taken as $\Gamma(J/\psi\to\ell^+\ell^-) = 5.53$ keV and $\Gamma(\psi(2S)\to\ell^+\ell^-) = 2.33$ keV [58].

Since the quarks are confined in hadron, the weak transition matrix element cannot be calculated in the framework of perturbative QCD. They are conventionally parametrized in terms of eight (axial-)vector and six (pseudo-)tensor type dimensionless form factors [21,25,31,32,59–61]. In this work, we adopt the helicity-based form as [31,32]

$$\begin{aligned}\langle\Lambda^*(k,s_{\Lambda^*})|\bar{s}\gamma^\mu b|\Lambda_b(p,s_{\Lambda_b})\rangle &= \bar{u}_\alpha(k,s_{\Lambda^*})\Big\{p^\alpha\Big[f_t^V(q^2)(m_{\Lambda_b}-m_{\Lambda^*})\frac{q^\mu}{q^2} + f_0^V(q^2)\frac{m_{\Lambda_b}+m_{\Lambda^*}}{s_+}\Big(p^\mu+k^\mu-(m_{\Lambda_b}^2-m_{\Lambda^*}^2)\frac{q^\mu}{q^2}\Big)\\ &\quad + f_\perp^V(q^2)\Big(\gamma^\mu - \frac{2m_{\Lambda^*}}{s_+}p^\mu - \frac{2m_{\Lambda_b}}{s_+}k^\mu\Big)\Big]\\ &\quad + f_g^V(q^2)\Big[g^{\alpha\mu} + m_{\Lambda^*}\frac{p^\alpha}{s_-}\Big(\gamma^\mu - \frac{2k^\mu}{m_{\Lambda^*}} + \frac{2(m_{\Lambda^*}p^\mu + m_{\Lambda_b}k^\mu)}{s_+}\Big)\Big]\Big\}u(p,s_{\Lambda_b}),\end{aligned} \tag{2.7}$$

$$\begin{aligned}\langle\Lambda^*(k,s_{\Lambda^*})|\bar{s}\gamma^\mu\gamma^5 b|\Lambda_b(p,s_{\Lambda_b})\rangle &= -\bar{u}_\alpha(k,s_{\Lambda^*})\gamma^5\Big\{p^\alpha\Big[f_t^A(q^2)(m_{\Lambda_b}+m_{\Lambda^*})\frac{q^\mu}{q^2} + f_0^A(q^2)\frac{m_{\Lambda_b}-m_{\Lambda^*}}{s_-}\Big(p^\mu+k^\mu-(m_{\Lambda_b}^2-m_{\Lambda^*}^2)\frac{q^\mu}{q^2}\Big)\\ &\quad + f_\perp^A(q^2)\Big(\gamma^\mu + \frac{2m_{\Lambda^*}}{s_-}p^\mu - \frac{2m_{\Lambda_b}}{s_-}k^\mu\Big)\Big]\\ &\quad + f_g^A(q^2)\Big[g^{\alpha\mu} - m_{\Lambda^*}\frac{p^\alpha}{s_+}\Big(\gamma^\mu + \frac{2k^\mu}{m_{\Lambda^*}} - \frac{2(m_{\Lambda^*}p^\mu - m_{\Lambda_b}k^\mu)}{s_-}\Big)\Big]\Big\}u(p,s_{\Lambda_b}),\end{aligned} \tag{2.8}$$

$$\begin{aligned}\langle\Lambda^*(k,s_{\Lambda^*})|\bar{s}i\sigma^{\mu\nu}q_\nu b|\Lambda_b(p,s_{\Lambda_b})\rangle &= -\bar{u}_\alpha(k,s_{\Lambda^*})\Big\{p^\alpha\Big[f_0^T(q^2)\frac{q^2}{s_+}\Big(p^\mu+k^\mu-(m_{\Lambda_b}^2-m_{\Lambda^*}^2)\frac{q^\mu}{q^2}\Big)\\ &\quad + f_\perp^T(q^2)(m_{\Lambda_b}+m_{\Lambda^*})\Big(\gamma^\mu - \frac{2m_{\Lambda^*}}{s_+}p^\mu - \frac{2m_{\Lambda_b}}{s_+}k^\mu\Big)\Big]\\ &\quad + f_g^T(q^2)\Big[g^{\alpha\mu} + m_{\Lambda^*}\frac{p^\alpha}{s_-}\Big(\gamma^\mu - \frac{2k^\mu}{m_{\Lambda^*}} + \frac{2(m_{\Lambda^*}p^\mu + m_{\Lambda_b}k^\mu)}{s_+}\Big)\Big]\Big\}u(p,s_{\Lambda_b}),\end{aligned} \tag{2.9}$$

$$\begin{aligned}\langle\Lambda^*(k,s_{\Lambda^*})|\bar{s}i\sigma^{\mu\nu}q_\nu\gamma^5 b|\Lambda_b(p,s_{\Lambda_b})\rangle &= -\bar{u}_\alpha(k,s_{\Lambda^*})\gamma^5\Big\{p^\alpha\Big[f_0^{T5}(q^2)\frac{q^2}{s_-}\Big(p^\mu+k^\mu-(m_{\Lambda_b}^2-m_{\Lambda^*}^2)\frac{q^\mu}{q^2}\Big)\\ &\quad + f_\perp^{T5}(q^2)(m_{\Lambda_b}-m_{\Lambda^*})\Big(\gamma^\mu + \frac{2m_{\Lambda^*}}{s_-}p^\mu - \frac{2m_{\Lambda_b}}{s_-}k^\mu\Big)\Big]\\ &\quad + f_g^{T5}(q^2)\Big[g^{\alpha\mu} - m_{\Lambda^*}\frac{p^\alpha}{s_+}\Big(\gamma^\mu + \frac{2k^\mu}{m_{\Lambda^*}} - \frac{2(m_{\Lambda^*}p^\mu - m_{\Lambda_b}k^\mu)}{s_-}\Big)\Big]\Big\}u(p,s_{\Lambda_b}).\end{aligned} \tag{2.10}$$

This form defined above is convenient for calculating the corresponding helicity amplitudes, where q^2 is the transferred momentum square and $s_\pm = (m_{\Lambda_b}\pm m_{\Lambda^*})^2 - q^2$.

A. The helicity amplitudes of the $\Lambda_b \to \Lambda^* \ell^+ \ell^-$ decay

To calculate the $\Lambda_b \to \Lambda^* \ell^+ \ell^-$ process, we define the corresponding helicity amplitudes of the $\Lambda_b(s_{\Lambda_b}) \to \Lambda^*(s_{\Lambda^*})$ transition as

$$H^{(V,A,T,T5)}(s_{\Lambda_b}, s_{\Lambda^*}, \lambda_W) = \epsilon^*_\mu(\lambda_W)\langle \Lambda^*(s_{\Lambda^*}) \times |\bar{s}\{\gamma^\mu, \gamma^\mu\gamma^5, i\sigma^{\mu\nu}q_\nu, i\sigma^{\mu\nu}q_\nu\gamma^5\} \times b|\Lambda_b(s_{\Lambda_b})\rangle, \tag{2.11}$$

where $\epsilon^\mu(\lambda_W = t, \pm, 0)$ are the polarization vectors of the virtual gauge boson in the Λ_b rest frame, and s_{Λ_b} and s_{Λ^*} are the polarizations of Λ_b and Λ^*, respectively. For the vector current, the complete helicity amplitudes $H^V(s_{\Lambda_b}, s_{\Lambda^*}, \lambda_W)$ read as [31]

$$H^V(s_{\Lambda_b}, s_{\Lambda^*}, t) = \epsilon^*_\mu(t)\langle \Lambda^*(k, s_{\Lambda^*})|\bar{s}\gamma^\mu b|\Lambda_b(p, s_{\Lambda_b})\rangle = f_t^V(q^2)\frac{m_{\Lambda_b} - m_{\Lambda^*}}{\sqrt{q^2}}\bar{u}_\alpha(k, s_{\Lambda^*})p^\alpha u(p, s_{\Lambda_b}), \tag{2.12}$$

$$H^V(s_{\Lambda_b}, s_{\Lambda^*}, 0) = \epsilon^*_\mu(0)\langle \Lambda^*(k, s_{\Lambda^*})|\bar{s}\gamma^\mu b|\Lambda_b(p, s_{\Lambda_b})\rangle = 2f_0^V(q^2)\frac{m_{\Lambda_b} + m_{\Lambda^*}}{s_+}k\cdot\epsilon^*(0) \times \bar{u}_\alpha(k, s_{\Lambda^*})p^\alpha u(p, s_{\Lambda_b}), \tag{2.13}$$

$$H^V(s_{\Lambda_b}, s_{\Lambda^*}, \pm) = \epsilon^*_\mu(\pm)\langle \Lambda^*(k, s_{\Lambda^*})|\bar{s}\gamma^\mu b|\Lambda_b(p, s_{\Lambda_b})\rangle = \left(f_\perp^V(q^2) + f_g^V(q^2)\frac{m_{\Lambda^*}}{s_-}\right)\bar{u}_\alpha(k, s_{\Lambda^*}) \times p^\alpha \not{\epsilon}^*(\pm)u(p, s_{\Lambda_b}) + f_g^V(q^2)\bar{u}_\alpha(k, s_{\Lambda^*})\epsilon^{*\alpha}(\pm)u(p, s_{\Lambda_b}). \tag{2.14}$$

Analogous expressions for the helicity amplitudes of the axial-vector, tensor, and pseudotensor currents are written as

$$H^A(s_{\Lambda_b}, s_{\Lambda^*}, t) = \epsilon^*_\mu(t)\langle \Lambda^*(k, s_{\Lambda^*})|\bar{s}\gamma^\mu\gamma^5 b|\Lambda_b(p, s_{\Lambda_b})\rangle = -f_t^A(q^2)\frac{m_{\Lambda_b} + m_{\Lambda^*}}{\sqrt{q^2}}\bar{u}_\alpha(k, s_{\Lambda^*}) \times p^\alpha\gamma^5 u(p, s_{\Lambda_b}), \tag{2.15}$$

$$H^A(s_{\Lambda_b}, s_{\Lambda^*}, 0) = \epsilon^*_\mu(0)\langle \Lambda^*(k, s_{\Lambda^*})|\bar{s}\gamma^\mu\gamma^5 b|\Lambda_b(p, s_{\Lambda_b})\rangle = -2f_0^A(q^2)\frac{m_{\Lambda_b} - m_{\Lambda^*}}{s_-}k\cdot\epsilon^*(0) \times \bar{u}_\alpha(k, s_{\Lambda^*})p^\alpha\gamma^5 u(p, s_{\Lambda_b}), \tag{2.16}$$

$$H^A(s_{\Lambda_b}, s_{\Lambda^*}, \pm) = \epsilon^*_\mu(\pm)\langle \Lambda^*(k, s_{\Lambda^*})|\bar{s}\gamma^\mu\gamma^5 b|\Lambda_b(p, s_{\Lambda_b})\rangle = \left(f_\perp^A(q^2) - f_g^A(q^2)\frac{m_{\Lambda^*}}{s_+}\right)\bar{u}_\alpha(k, s_{\Lambda^*}) \times p^\alpha \not{\epsilon}^*(\pm)\gamma^5 u(p, s_{\Lambda_b}) - f_g^A(q^2)\bar{u}_\alpha(k, s_{\Lambda^*})\epsilon^{*\alpha}(\pm)\gamma^5 u(p, s_{\Lambda_b}), \tag{2.17}$$

$$H^T(s_{\Lambda_b}, s_{\Lambda^*}, 0) = \epsilon^*_\mu(0)\langle \Lambda^*(k, s_{\Lambda^*})|\bar{s}i\sigma^{\mu\nu}q_\nu b|\Lambda_b(p, s_{\Lambda_b})\rangle = -2f_0^T(q^2)\frac{q^2}{s_+}k\cdot\epsilon^*(0) \times \bar{u}_\alpha(k, s_{\Lambda^*})p^\alpha u(p, s_{\Lambda_b}), \tag{2.18}$$

$$H^T(s_{\Lambda_b}, s_{\Lambda^*}, \pm) = \epsilon^*_\mu(\pm)\langle \Lambda^*(k, s_{\Lambda^*})|\bar{s}i\sigma^{\mu\nu}q_\nu b|\Lambda_b(p, s_{\Lambda_b})\rangle = -\left(f_\perp^T(q^2)(m_{\Lambda_b} + m_{\Lambda^*}) + f_g^T(q^2)\frac{m_{\Lambda^*}}{s_-}\right) \times \bar{u}_\alpha(k, s_{\Lambda^*})p^\alpha \not{\epsilon}^*(\pm)u(p, s_{\Lambda_b}) - f_g^T(q^2)\bar{u}_\alpha(k, s_{\Lambda^*})\epsilon^{*\alpha}(\pm)u(p, s_{\Lambda_b}), \tag{2.19}$$

$$H^{T5}(s_{\Lambda_b}, s_{\Lambda^*}, 0) = \epsilon^*_\mu(0)\langle \Lambda^*(k, s_{\Lambda^*})|\bar{s}i\sigma^{\mu\nu}q_\nu\gamma^5 b|\Lambda_b(p, s_{\Lambda_b})\rangle = -2f_0^{T5}(q^2)\frac{q^2}{s_-}k\cdot\epsilon^*(0) \times \bar{u}_\alpha(k, s_{\Lambda^*})p^\alpha\gamma^5 u(p, s_{\Lambda_b}), \tag{2.20}$$

$$H^{T5}(s_{\Lambda_b}, s_{\Lambda^*}, \pm) = \epsilon^*_\mu(\pm)\langle \Lambda^*(k, s_{\Lambda^*})|\bar{s}i\sigma^{\mu\nu}q_\nu\gamma^5 b|\Lambda_b(p, s_{\Lambda_b})\rangle = \left(f_\perp^{T5}(q^2)(m_{\Lambda_b} - m_{\Lambda^*}) - f_g^{T5}(q^2)\frac{m_{\Lambda^*}}{s_+}\right) \times \bar{u}_\alpha(k, s_{\Lambda^*})p^\alpha \not{\epsilon}^*(\pm)\gamma^5 u(p, s_{\Lambda_b}) - f_g^{T5}(q^2)\bar{u}_\alpha(k, s_{\Lambda^*})\epsilon^{*\alpha}(\pm)\gamma^5 u(p, s_{\Lambda_b}), \tag{2.21}$$

respectively. Using the kinematic conventions presented in Appendix B 1, the nonzero terms for the above helicity amplitudes of the vector, axial-vector, tensor, and pseudotensor currents are [31]

$$
\begin{aligned}
H^V(+1/2,+1/2,t) &= H^V(-1/2,-1/2,t) = f_t^V(q^2)\frac{m_{\Lambda_b}-m_{\Lambda^*}}{\sqrt{q^2}}\frac{s_+\sqrt{s_-}}{\sqrt{6}m_{\Lambda^*}},\\
H^V(+1/2,+1/2,0) &= H^V(-1/2,-1/2,0) = -f_0^V(q^2)\frac{m_{\Lambda_b}+m_{\Lambda^*}}{\sqrt{q^2}}\frac{s_-\sqrt{s_+}}{\sqrt{6}m_{\Lambda^*}},\\
H^V(+1/2,-1/2,+) &= H^V(-1/2,+1/2,-) = -f_\perp^V(q^2)\frac{s_-\sqrt{s_+}}{\sqrt{3}m_{\Lambda^*}},\\
H^V(-1/2,-3/2,+) &= H^V(+1/2,+3/2,-) = f_g^V(q^2)\sqrt{s_+},
\end{aligned}
\tag{2.22}
$$

$$
\begin{aligned}
H^A(+1/2,+1/2,t) &= -H^A(-1/2,-1/2,t) = f_t^A(q^2)\frac{m_{\Lambda_b}+m_{\Lambda^*}}{\sqrt{q^2}}\frac{s_-\sqrt{s_+}}{\sqrt{6}m_{\Lambda^*}},\\
H^A(+1/2,+1/2,0) &= -H^A(-1/2,-1/2,0) = -f_0^A(q^2)\frac{m_{\Lambda_b}-m_{\Lambda^*}}{\sqrt{q^2}}\frac{s_+\sqrt{s_-}}{\sqrt{6}m_{\Lambda^*}},\\
H^A(+1/2,-1/2,+) &= -H^A(-1/2,+1/2,-) = f_\perp^A(q^2)\frac{s_+\sqrt{s_-}}{\sqrt{3}m_{\Lambda^*}},\\
H^A(-1/2,-3/2,+) &= -H^A(+1/2,+3/2,-) = -f_g^A(q^2)\sqrt{s_-},
\end{aligned}
\tag{2.23}
$$

$$
\begin{aligned}
H^T(+1/2,+1/2,0) &= H^T(-1/2,-1/2,0) = f_0^T(q^2)\sqrt{q^2}\frac{s_-\sqrt{s_+}}{\sqrt{6}m_{\Lambda^*}},\\
H^T(+1/2,-1/2,+) &= H^T(-1/2,+1/2,-) = f_\perp^T(q^2)(m_{\Lambda_b}+m_{\Lambda^*})\frac{s_-\sqrt{s_+}}{\sqrt{3}m_{\Lambda^*}},\\
H^T(-1/2,-3/2,+) &= H^T(+1/2,+3/2,-) = -f_g^T(q^2)\sqrt{s_+},
\end{aligned}
\tag{2.24}
$$

$$
\begin{aligned}
H^{T5}(+1/2,+1/2,0) &= -H^{T5}(-1/2,-1/2,0) = -f_0^{T5}(q^2)\sqrt{q^2}\frac{s_+\sqrt{s_-}}{\sqrt{6}m_{\Lambda^*}},\\
H^{T5}(+1/2,-1/2,+) &= -H^{T5}(-1/2,+1/2,-) = f_\perp^{T5}(q^2)(m_{\Lambda_b}-m_{\Lambda^*})\frac{s_+\sqrt{s_-}}{\sqrt{3}m_{\Lambda^*}},\\
H^{T5}(-1/2,-3/2,+) &= -H^{T5}(+1/2,+3/2,-) = -f_g^{T5}(q^2)\sqrt{s_-},
\end{aligned}
\tag{2.25}
$$

respectively.

Similarly, we define the leptonic helicity amplitudes as

$$
\begin{aligned}
L^{(V,A)}(s_{\ell^-},s_{\ell^+},\lambda_W) &= \bar{\epsilon}^\mu(\lambda_W)\langle \ell^-\ell^+|\bar{\ell}^-\{\gamma_\mu,\gamma_\mu\gamma^5\}\ell^+|0\rangle\\
&= \bar{\epsilon}^\mu(\lambda_W)\bar{u}(p_\ell,s_{\ell^-})\{\gamma_\mu,\gamma_\mu\gamma^5\}v(-p_\ell,s_{\ell^+}),
\end{aligned}
\tag{2.26}
$$

where $\bar{\epsilon}^\mu(\lambda_W = t,\pm,0)$ are the polarization vectors of the virtual gauge boson in the dilepton rest frame. Using the kinematic conventions presented in Appendix B 2, the nonzero terms are obtained as [32]

$$
\begin{aligned}
L^V(\pm1/2,\pm1/2,0) &= \pm 2m_\ell\cos\theta_\ell, \qquad L^V(\pm1/2,\mp1/2,0) = -\sqrt{q^2}\sin\theta_\ell,\\
L^V(+1/2,+1/2,\pm) &= \mp\sqrt{2}m_\ell\sin\theta_\ell, \qquad L^V(-1/2,-1/2,\mp) = \mp\sqrt{2}m_\ell\sin\theta_\ell,\\
L^V(\pm1/2,\mp1/2,\pm) &= \mp\frac{\sqrt{q^2}}{\sqrt{2}}(1+\cos\theta_\ell), \qquad L^V(\pm1/2,\mp1/2,\mp) = \mp\frac{\sqrt{q^2}}{\sqrt{2}}(1-\cos\theta_\ell),\\
L^A(\pm1/2,\pm1/2,t) &= -2m_\ell, \qquad L^A(\pm1/2,\mp1/2,0) = \mp\sin\theta_\ell\sqrt{q^2}\beta_\ell,\\
L^A(\pm1/2,\mp1/2,\pm) &= -\frac{\sqrt{q^2}}{\sqrt{2}}(1+\cos\theta_\ell)\beta_\ell, \qquad L^A(\pm1/2,\mp1/2,\mp) = -\frac{\sqrt{q^2}}{\sqrt{2}}(1-\cos\theta_\ell)\beta_\ell,
\end{aligned}
\tag{2.27}
$$

where $\beta_\ell \equiv \sqrt{1-4m_\ell^2/q^2}$.

B. The helicity amplitudes of the $\Lambda^* \to N\bar{K}$ decay

We use the effective Lagrangian approach to describe the strong decay process $\Lambda^* \to N\bar{K}$. The concerned effective Lagrangian is

$$\mathcal{L}_{\Lambda^* KN} = g_{\Lambda^* KN} \bar{N} \gamma_5 \Lambda^*_\alpha \partial^\alpha K, \tag{2.28}$$

where $g_{\Lambda^* KN}$ is the coupling constant. So the decay amplitude for the $\Lambda^* \to N\bar{K}$ process can be expressed as

$$\mathcal{M}_{\Lambda^* \to N\bar{K}}(s_{\Lambda^*}, s_N) = g_{\Lambda^* KN} \bar{u}_N(s_N) \gamma_5 u_{\Lambda^*,\alpha}(s_{\Lambda^*}) k_2^\alpha, \tag{2.29}$$

where k_2^α is the four momentum of the K meson, $u_{\Lambda^*,\alpha}$ is the Rarita-Schwinger spinor describing the hyperon Λ^*, while u_N is the Dirac spinor describing the nucleon. The interference terms between matrix elements with different Λ^* polarizations can be written as

$$\Gamma_{\Lambda^* \to N\bar{K}}(s^a_{\Lambda^*}, s^b_{\Lambda^*}) = \frac{\sqrt{r_- r_+}}{16\pi m^3_{\Lambda^*}} \sum_{s_N} \left[\mathcal{M}_{\Lambda^* \to N\bar{K}}(s^b_{\Lambda^*}, s_N)\right]^* \times \mathcal{M}_{\Lambda^* \to N\bar{K}}(s^a_{\Lambda^*}, s_N), \tag{2.30}$$

where $r_\pm = (m_{\Lambda^*} \pm m_N)^2 - m_K^2$, and then the decay width of $\Lambda^* \to N\bar{K}$ can be obtained by

$$\Gamma(\Lambda^* \to N\bar{K}) = \frac{1}{4} \sum_{s_{\Lambda^*}} \Gamma_{\Lambda^* \to N\bar{K}}(s_{\Lambda^*}, s_{\Lambda^*}), \tag{2.31}$$

where the factor 4 comes from averaging over the polarization of Λ^*.

With respect to the forms of Rarita-Schwinger spinors and Dirac spinors presented in Appendix B 3, we obtain [31,32]

$$\Gamma_{\Lambda^* \to N\bar{K}}(s^a_{\Lambda^*}, s^b_{\Lambda^*}) = \frac{\Gamma(\Lambda^* \to N\bar{K})}{4} \begin{pmatrix} 6\sin^2(\theta_{\Lambda^*}) & 2\sqrt{3}e^{-i\phi}\sin(2\theta_{\Lambda^*}) & -2\sqrt{3}e^{-2i\phi}\sin^2(\theta_{\Lambda^*}) & 0 \\ 2\sqrt{3}e^{i\phi}\sin(2\theta_{\Lambda^*}) & 3\cos(2\theta_{\Lambda^*})+5 & 0 & -2\sqrt{3}e^{-2i\phi}\sin^2(\theta_{\Lambda^*}) \\ -2\sqrt{3}e^{2i\phi}\sin^2(\theta_{\Lambda^*}) & 0 & 3\cos(2\theta_{\Lambda^*})+5 & -2\sqrt{3}e^{-i\phi}\sin(2\theta_{\Lambda^*}) \\ 0 & -2\sqrt{3}e^{2i\phi}\sin^2(\theta_{\Lambda^*}) & -2\sqrt{3}e^{i\phi}\sin(2\theta_{\Lambda^*}) & 6\sin^2(\theta_{\Lambda^*}) \end{pmatrix}, \tag{2.32}$$

with rows and columns corresponding to the polarizations of $s^a_{\Lambda^*}, s^b_{\Lambda^*} = -3/2, -1/2, 1/2, 3/2$ from top to bottom and from left to right. We emphasize that $\Gamma(\Lambda^* \to N\bar{K}) = \mathcal{B}_{\Lambda^*} \times \Gamma_{\Lambda^*}$, where $\mathcal{B}_{\Lambda^*} \equiv \mathcal{B}(\Lambda^* \to N\bar{K})$ is the corresponding branching ratio and Γ_{Λ^*} is the inclusive decay width of the Λ^* hyperon.

C. The total amplitudes of $\Lambda_b \to \Lambda^*(\to N\bar{K})\ell^+\ell^-$ process

The invariant amplitude of $\Lambda_b \to \Lambda^*(\to N\bar{K})\ell^+\ell^-$ is [24]

$$\begin{aligned}
\mathcal{M}(s_{\Lambda_b}, s_N, s_{\ell^-}, s_{\ell^+}) &= \langle N(s_N)\bar{K}\ell^-(s_{\ell^-})\ell^+(s_{\ell^+})|\mathcal{H}_{\rm eff}|\Lambda_b(s_{\Lambda_b})\rangle \\
&= \sum_{s_{\Lambda^*}} \frac{i}{k^2 - m^2_{\Lambda^*}} \mathcal{M}_{\Lambda^* \to N\bar{K}}(s_{\Lambda^*}, s_N) \langle \Lambda^*(s^*_\Lambda)\ell^-(s_{\ell^-})\ell^+(s_{\ell^+})|\mathcal{H}_{\rm eff}|\Lambda_b(s_{\Lambda_b})\rangle \\
&= \sum_{s_{\Lambda^*}} \frac{iN}{2(k^2 - m^2_{\Lambda^*})} \mathcal{M}_{\Lambda^* \to N\bar{K}}(s_{\Lambda^*}, s_N) g^{\mu\nu} \langle \Lambda^*(s_{\Lambda^*})|j_\mu|\Lambda_b(s_{\Lambda_b})\rangle \langle \ell^-(s_{\ell^-})\ell^+(s_{\ell^+})|j_\nu|0\rangle \\
&= \sum_{s_{\Lambda^*}} \frac{iN}{2(k^2 - m^2_{\Lambda^*})} \mathcal{M}_{\Lambda^* \to N\bar{K}}(s_{\Lambda^*}, s_N) \Big[C_9^{\rm eff} H^V(s_{\Lambda_b}, s_{\Lambda^*}, t) L^V(s_{\ell^-}, s_{\ell^+}, t) - C_9^{\rm eff} H^A(s_{\Lambda_b}, s_{\Lambda^*}, t) \\
&\quad \times L^V(s_{\ell^-}, s_{\ell^+}, t) + C_{10} H^V(s_{\Lambda_b}, s_{\Lambda^*}, t) L^A(s_{\ell^-}, s_{\ell^+}, t) - C_{10} H^A(s_{\Lambda_b}, s_{\Lambda^*}, t) L^A(s_{\ell^-}, s_{\ell^+}, t) \\
&\quad - \frac{2m_b}{q^2} C_7^{\rm eff} H^T(s_{\Lambda_b}, s_{\Lambda^*}, t) L^V(s_{\ell^-}, s_{\ell^+}, t) - \frac{2m_b}{q^2} C_7^{\rm eff} H^{T5}(s_{\Lambda_b}, s_{\Lambda^*}, t) L^V(s_{\ell^-}, s_{\ell^+}, t) \\
&\quad - \sum_{\lambda=\pm,0} \Big(C_9^{\rm eff} H^V(s_{\Lambda_b}, s_{\Lambda^*}, \lambda) L^V(s_{\ell^-}, s_{\ell^+}, \lambda) - C_9^{\rm eff} H^A(s_{\Lambda_b}, s_{\Lambda^*}, \lambda) L^V(s_{\ell^-}, s_{\ell^+}, \lambda) \\
&\quad + C_{10} H^V(s_{\Lambda_b}, s_{\Lambda^*}, \lambda) L^A(s_{\ell^-}, s_{\ell^+}, \lambda) - C_{10} H^A(s_{\Lambda_b}, s_{\Lambda^*}, \lambda) L^A(s_{\ell^-}, s_{\ell^+}, \lambda) \\
&\quad - \frac{2m_b}{q^2} C_7^{\rm eff} H^T(s_{\Lambda_b}, s_{\Lambda^*}, \lambda) L^V(s_{\ell^-}, s_{\ell^+}, \lambda) - \frac{2m_b}{q^2} C_7^{\rm eff} H^{T5}(s_{\Lambda_b}, s_{\Lambda^*}, \lambda) L^V(s_{\ell^-}, s_{\ell^+}, \lambda) \Big) \Big],
\end{aligned} \tag{2.33}$$

where $N \equiv \frac{4G_F}{\sqrt{2}} V_{tb} V_{ts}^* \frac{\alpha_e}{4\pi}$, and the factor $1/2$ comes from the definition of $P_{L(R)}$. Besides, the relation $g^{\mu\nu} = \epsilon_t^{*\mu}\epsilon_t^{\nu} - \sum_{\lambda=\pm,0} \epsilon_\lambda^{*\mu}\epsilon_\lambda^{\nu}$ is implied. The helicity amplitudes defined in Eqs. (2.11), (2.26), (2.30), and (2.32) are implied. Finally, with the nonzero helicity amplitudes presented in Eqs. (2.22)–(2.25), (2.27), and (2.32), and the expression of the differential width by considering the narrow-width approximation shown in Eq. (A7), the differential decay width can be obtained.

As analyzed in Refs. [31,32], the angular distribution for the four-body decay $\Lambda_b \to \Lambda^*(\to N\bar{K})\ell^+\ell^-$ can be reduced as

$$\begin{aligned}\frac{d^4\Gamma}{dq^2 d\cos\theta_{\Lambda^*} d\cos\theta_\ell d\phi} &= \frac{3}{8\pi}\sum_i L_i(q^2) f_i(q^2,\theta_\ell,\theta_{\Lambda^*},\phi) \\ &= \frac{3}{8\pi}\Big[(L_{1c}\cos\theta_\ell + L_{1cc}\cos^2\theta_\ell + L_{1ss}\sin^2\theta_\ell)\cos^2\theta_{\Lambda^*} \\ &\quad + (L_{2c}\cos\theta_\ell + L_{2cc}\cos^2\theta_\ell + L_{2ss}\sin^2\theta_\ell)\sin^2\theta_{\Lambda^*} \\ &\quad + (L_{3ss}\sin^2\theta_\ell\cos^2\phi + L_{4ss}\sin^2\theta_\ell\sin\phi\cos\phi)\sin^2\theta_{\Lambda^*} \\ &\quad + (L_{5s}\sin\theta_\ell + L_{5sc}\sin\theta_\ell\cos\theta_\ell)\sin\theta_{\Lambda^*}\cos\theta_{\Lambda^*}\cos\phi \\ &\quad + (L_{6s}\sin\theta_\ell + L_{6sc}\sin\theta_\ell\cos\theta_\ell)\sin\theta_{\Lambda^*}\cos\theta_{\Lambda^*}\sin\phi\Big]. \end{aligned} \tag{2.34}$$

The complete expressions for the series angular coefficients L_i can be found in Appendix G of Ref. [32].

D. Physical observable in the four-body process

By integrating over the angles in the regions $\theta_\ell \in [0,\pi]$, $\theta_\Lambda \in [0,\pi]$, and $\phi \in [0,2\pi]$, the relevant physical observables are listed as follows:

(a) The differential width is

$$\begin{aligned}\frac{d\Gamma}{dq^2} &= \int_{-1}^{1} d\cos\theta_\ell \int_{-1}^{1} d\cos\theta_{\Lambda^*} \int_0^{2\pi} d\phi \frac{d\Gamma}{dq^2 d\cos\theta_{\Lambda^*} d\cos\theta_\ell d\phi} \\ &= \frac{1}{3}(L_{1cc} + 2L_{1ss} + 2L_{2cc} + 4L_{2ss} + 2L_{3ss}). \end{aligned} \tag{2.35}$$

(b) The lepton-side forward-backward symmetry A_{FB}^{ℓ} is

$$\begin{aligned} A_{FB}^{\ell} &= \frac{\left(\int_{-1}^{0} - \int_{0}^{1}\right) d\cos\theta_\ell \int_{-1}^{1} d\cos\theta_{\Lambda^*} \int_0^{2\pi} d\phi \frac{d\Gamma}{dq^2 d\cos\theta_{\Lambda^*} d\cos\theta_\ell d\phi}}{\int_{-1}^{1} d\cos\theta_\ell \int_{-1}^{1} d\cos\theta_{\Lambda^*} \int_0^{2\pi} d\phi \frac{d\Gamma}{dq^2 d\cos\theta_{\Lambda^*} d\cos\theta_\ell d\phi}} \\ &= \frac{3}{2}\frac{L_{1c} + 2L_{2c}}{L_{1cc} + 2L_{1ss} + 2L_{2cc} + 4L_{2ss} + 2L_{3ss}}. \end{aligned} \tag{2.36}$$

(c) The hadron-side forward-backward symmetry $A_{FB}^{\Lambda^*}$ and the lepton-hadron-side forward-backward symmetry $A_{FB}^{\ell\Lambda^*}$ will undoubtedly disappear, since the decay $\Lambda^* \to N\bar{K}$ is a strong process [31]. This can be tested in future experiments.

(d) The transverse and longitudinal polarization fractions of the dilepton system are defined as [31]

$$F_T = \frac{2(L_{1cc} + 2L_{2cc})}{L_{1cc} + 2(L_{1ss} + L_{2cc} + 2L_{2ss} + L_{3ss})}, \tag{2.37}$$

$$F_L = 1 - \frac{2(L_{1cc} + 2L_{2cc})}{L_{1cc} + 2(L_{1ss} + L_{2cc} + 2L_{2ss} + L_{3ss})}, \tag{2.38}$$

respectively.

(e) We also define the normalized angular observables as

$$\langle A\rangle_{[q^2_{\rm min}, q^2_{\rm max}]} = \left[\int_{q^2_{\rm min}}^{q^2_{\rm max}} A[q^2]\frac{d\Gamma}{dq^2}dq^2\right] \Big/ \left[\int_{q^2_{\rm min}}^{q^2_{\rm max}} \frac{d\Gamma}{dq^2}dq^2\right] \tag{2.39}$$

with $A[q^2] = A_{FB}^{\ell}[q^2]$, $F_T[q^2]$, or $F_L[q^2]$.

III. THE LIGHT-FRONT QUARK MODEL FOR CALCULATING WEAK TRANSITION FORM FACTORS

In this section, we will calculate the form factors involved in the three-body light-front quark model. First, the vertex function of a baryon $\mathcal{B}$ with spin J and momentum P is [42,43,62–67]

$$\begin{aligned}|\mathcal{B}(P,J,J_z)\rangle = &\int \frac{d^3\tilde{p}_1}{2(2\pi)^3}\frac{d^3\tilde{p}_2}{2(2\pi)^3}\frac{d^3\tilde{p}_3}{2(2\pi)^3}2(2\pi)^3 \\ &\times \sum_{\lambda_1,\lambda_2,\lambda_3}\Psi^{J,J_z}(\tilde{p}_i,\lambda_i)C^{\alpha\beta\gamma}\delta^3(\tilde{P}-\tilde{p}_1-\tilde{p}_2-\tilde{p}_3) \\ &\times F_{q_1q_2q_3}|q_{1\alpha}(\tilde{p}_1,\lambda_1)\rangle|q_{2\beta}(\tilde{p}_2,\lambda_2)\rangle \\ &\times|q_{3\gamma}(\tilde{p}_3,\lambda_3)\rangle, \end{aligned} \tag{3.1}$$

where the $C^{\alpha\beta\gamma}$ and $F_{q_1q_2q_3}$ are the color and flavor factors, respectively, and λ_i and p_i $(i = 1,2,3)$ are the helicities and light-front momenta of the on-mass-shell quarks, respectively, defined as

$$\tilde{p}_i = (p_i^+, \vec{p}_{i\perp}), \quad p_i^+ = p_i^0 + p_i^3, \quad \vec{p}_{i\perp} = (p_i^1, p_i^2). \tag{3.2}$$

To describe the motion of the constituents, the intrinsic variables $(x_i, \vec{k}_i)$ $(i = 1, 2, 3)$ are as follows:

$$\begin{aligned} &p_i^+ = x_i P^+, \qquad \vec{p}_{i\perp} = x_i\vec{P}_{i\perp} + \vec{k}_{i\perp}, \\ &\sum_{i=1}^{3}\vec{k}_{i\perp} = 0, \qquad \sum_{i=1}^{3}x_i = 1, \end{aligned} \tag{3.3}$$

where x_i represents the light-front momentum fractions bounded by $0 < x_i < 1$.

The vertex function should be normalized by

$$\langle\mathcal{B}(P',J,J_z')|\mathcal{B}(P,J,J_z)\rangle = 2(2\pi)^3P^+\delta^3(\tilde{P}-\tilde{P}')\delta_{J_z,J_z'}, \tag{3.4}$$

and

$$\begin{aligned}\int\left(\prod_{i=1}^{3}\frac{dx_i d^2\vec{k}_{i\perp}}{2(2\pi)^3}\right)&2(2\pi)^3\delta\left(1-\sum_i x_i\right) \\ &\times\delta^2\left(\sum_i\vec{k}_{i\perp}\right)\psi^*(x_i,\vec{k}_{i\perp})\psi(x_i,\vec{k}_{i\perp}) = 1. \end{aligned} \tag{3.5}$$

As proposed by Refs. [68–70], the spin-spatial wave functions for the Λ-type baryon with $J^P = 1/2^+$ and $3/2^-$ are written as

$$\begin{aligned}\Psi^{1/2,J_z}(\tilde{p}_i,\lambda_i) = &A_0\bar{u}(p_1,\lambda_1)[(\not{P}+M_0)\gamma^5]v(p_2,\lambda_2) \\ &\times\bar{u}_Q(p_3,\lambda_3)u(P,J_z)\psi(x_i,\vec{k}_{i\perp}), \end{aligned} \tag{3.6}$$

$$\begin{aligned}\Psi^{3/2,J_z}(\tilde{p}_i,\lambda_i) = &B_0\bar{u}(p_1,\lambda_1)[(\not{P}+M_0)\gamma^5]v(p_2,\lambda_2) \\ &\times\bar{u}_Q(p_3,\lambda_3)K^\alpha u_\alpha(P,J_z)\psi(x_i,\vec{k}_{i\perp}), \end{aligned} \tag{3.7}$$

respectively, where

$$A_0 = \frac{1}{\sqrt{16P^+M_0^3(e_1+m_1)(e_2+m_2)(e_3+m_3)}},$$

$$B_0 = \frac{\sqrt{3}}{\sqrt{16P^+M_0^3(e_1+m_1)(e_2+m_2)(e_3-m_3)(e_3+m_3)^2}}$$

are the corresponding normalized factors determined by Eq. (3.4). The $K = [(m_1+m_2)p_3 - m_3(p_1+p_2)]/(m_1+m_2+m_3)$ is the momentum of the λ mode.

In the context of the three-body light-front quark model, the general expression for the weak transition matrix element is written as

$$\begin{aligned}\langle\Lambda^*(P',J_z')|\bar{s}\Gamma_i^\mu b|\Lambda_b(P,J_z)\rangle = &\int\left(\frac{dx_1d^2\vec{k}_{1\perp}}{2(2\pi)^3}\right)\left(\frac{dx_2d^2\vec{k}_{2\perp}}{2(2\pi)^3}\right)\frac{\psi_b(x_i,\vec{k}_{i\perp})\psi_s^*(x_i',\vec{k}_{i\perp}')}{(16/\sqrt{3})\sqrt{x_3x_3'M_0^3M_0'^3}} \\ &\times\frac{\mathrm{Tr}[(\not{P}'-M_0')\gamma^5(\not{p}_1+m_1)(\not{P}+M_0)\gamma^5(\not{p}_2-m_2)]}{\sqrt{(e_1+m_1)(e_2+m_2)(e_3+m_3)(e_1'+m_1')(e_2'+m_2')(e_3'-m_3')(e_3'+m_3')^2}} \\ &\times\bar{u}_\alpha(P',J_z')K'^\alpha(\not{p}_3'+m_3')\Gamma_i^\mu(\not{p}_3+m_3)u(P,J_z), \end{aligned} \tag{3.8}$$

where the $\Gamma_i^\mu = \{\gamma^\mu, \gamma^\mu\gamma^5, i\sigma^{\mu\nu}q_\nu, i\sigma^{\mu\nu}q_\nu\gamma^5\}$. $P = p_1+p_2+p_3$ and $P' = p_1+p_2+p_3'$ are the light-front momenta for initial and final baryons, respectively, considering $p_1 \equiv p_1'$ and $p_2 \equiv p_2'$ in the spectator scheme. The following kinematics of the constituent quarks as

$$p_i^{(\prime)+} = x_i^{(\prime)} P^{(\prime)+}, \qquad \vec{p}_{i\perp}^{(\prime)} = x_i^{(\prime)} \vec{P}_{i\perp}^{(\prime)} + \vec{k}_{i\perp}^{(\prime)},$$
$$p_3^+ - p_3'^+ = q^+, \qquad \vec{p}_{3\perp} - \vec{p}'_{3\perp} = \vec{q}_\perp,$$
$$\sum_{i=1}^{3} \vec{k}_{i\perp}^{(\prime)} = 0, \qquad \sum_{i=1}^{3} x_i^{(\prime)} = 1 \tag{3.9}$$

have been used to simplify the above matrix element.

In addition, the ψ_b and ψ_s are the spatial wave functions of Λ_b and Λ^*, respectively. Their forms are written as

$$\psi(x_i, \vec{k}_i) = N_\psi \sqrt{\frac{e_1 e_2 e_3}{x_1 x_2 x_3 M_0}} \phi_\rho\left(\frac{m_1 \vec{k}_2 - m_2 \vec{k}_1}{m_1 + m_2}\right) \times \phi_\lambda\left(\frac{(m_1 + m_2)\vec{k}_3 - m_3(\vec{k}_1 + \vec{k}_2)}{m_1 + m_2 + m_3}\right) \tag{3.10}$$

in this paper, where $\vec{k}_i = (\vec{k}_{i\perp}, k_{iz})$ with

$$k_{iz} = \frac{x_i M_0}{2} - \frac{m_i^2 + \vec{k}_{i\perp}^2}{2 x_i M_0}. \tag{3.11}$$

By the way, $\phi_{\rho(\lambda)}$ is the spatial wave function of $\rho(\lambda)$ mode. The factor $N_\psi = (4\pi^{3/2})^2$ for the ground state Λ_b and the factor $N_\psi = (4\pi^{3/2})^2/\sqrt{3}$ for the P-wave state $\Lambda(1520)$ are determined by Eq. (3.5). The additional factor $/1\sqrt{3}$ for the P-wave state comes from different angular components of the spatial wave functions described by the spherical harmonic functions compared to the ground state.

In previous work [40–42], the spatial wave function of the baryon is usually adopted as a SHO form with an oscillator parameter β, which causes the β dependence of the form factors. To avoid this uncertainty, we adopt the numerical spatial wave function obtained by solving the three-body Schrödinger equation with the semirelativistic potential model. The detailed discussions are presented in Sec. IV.

The next content discusses how to extract the form factors in the light-front quark model. Here, we consider the $q^+ = 0$ and $\vec{q}_\perp \neq 0$ condition. In order to extract the four form factors in vector current, one can multiply the $\bar{u}(P, J_z)\Gamma_i^{V,\mu\beta} u_\beta(P', J'_z)$ on both sides of Eq. (3.8) with specific setting $\Gamma_i^\mu = \gamma^\mu$ and sum over the polarizations of the initial and final states. And then the left side can be replaced by Eq. (2.7), and the right side can be calculated out by carrying out the traces and then the integration. The Lorentz structures are $\Gamma_i^{V,\mu\beta} = \{g^{\beta\mu}, P^\beta \gamma^\mu, P^\beta P'^\mu, P^\beta P^\mu\}$. The complete expressions for the form factors in vector current are obtained by solving

$$\begin{aligned}&\mathrm{Tr}[(G_{\Lambda^*})^{\beta\alpha}.[\text{form factors in Eq.(2.7)}].(\not{P} + M_0).\Gamma^{V,\beta}_{(1,2,3,4),\mu}] \\ &= \int \left(\frac{dx_1 d^2\vec{k}_{1\perp}}{2(2\pi)^3}\right)\left(\frac{dx_2 d^2\vec{k}_{2\perp}}{2(2\pi)^3}\right) \frac{\psi_b(x_i, \vec{k}_{i\perp})\psi_s^*(x'_i, \vec{k}'_{i\perp})}{\sqrt{x_3 x'_3}} A_0 B'_0 \mathrm{Tr}[\cdots] \\ &\quad \times \mathrm{Tr}[(G_{\Lambda^*})_{\beta\alpha} K'^\alpha (\not{p}'_3 + m'_3)\gamma^\mu (\not{p}_3 + m_3)(\not{P} + M_0)\Gamma^{V,\beta}_{(1,2,3,4),\mu}],\end{aligned} \tag{3.12}$$

where

$$A_0 = 1/\sqrt{16 M_0^3 (e_1 + m_1)(e_2 + m_2)(e_3 + m_3)}, \tag{3.13}$$

$$B'_0 = \sqrt{3}/\sqrt{16 M_0'^3 (e'_1 + m'_1)(e'_2 + m'_2)(e'_3 - m'_3)(e'_3 + m'_3)^2}, \tag{3.14}$$

$$\mathrm{Tr}[\cdots] = \mathrm{Tr}[(\not{P}' - M'_0)\gamma^5 (\not{p}_1 + m_1)(\not{P} - M_0)\gamma^5 (\not{p}_2 - m_2)], \tag{3.15}$$

$$(G_{\Lambda^*})^{\mu\nu} = -(\not{P}' + M'_0)\left[g^{\mu\nu} - \frac{1}{3}\gamma^\mu\gamma^\nu - \frac{2}{3M_0'^2} P'^\mu P'^\nu - \frac{1}{3M'_0}(\gamma^\mu P'^\nu - \gamma^\nu P'^\mu)\right]. \tag{3.16}$$

Analogously, the form factors in the axial-vector, tensor, and pseudotensor currents can be obtained by using the structures $\bar{u}(P, J_z)\Gamma_i^{A,\mu\beta} u_\beta(P', J'_z)$, $\bar{u}(P, J_z)\Gamma_i^{T,\mu\beta} u_\beta(P', J'_z)$, and $\bar{u}(P, J_z)\Gamma_i^{T5,\mu\beta} u_\beta(P', J'_z)$ with setting $\Gamma_i^\mu = \gamma^\mu\gamma^5$, $i\sigma^{\mu\nu}q_\nu$ and $i\sigma^{\mu\nu}q_\nu\gamma^5$ in Eq. (3.8), respectively. The Lorentz structures are $\Gamma_i^{A,\mu\beta} = \{g^{\beta\mu}\gamma^5, P^\beta\gamma^\mu\gamma^5, P^\beta P'^\mu\gamma^5, P^\beta P^\mu\gamma^5\}$, $\Gamma_i^{T,\mu\beta} = \{g^{\beta\mu}, P^\beta\gamma^\mu, P^\beta P'^\mu\}$, and $\Gamma_i^{T5,\mu\beta} = \{g^{\beta\mu}\gamma^5, P^\beta\gamma^\mu\gamma^5, P^\beta P'^\mu\gamma^5\}$. The complete expressions of the form factors can be obtained by solving

$$\begin{aligned}&\mathrm{Tr}[(G_{\Lambda^*})^{\beta\alpha}.[\text{form factors in Eq.(2.8)}].(\not{P}+M_0).\Gamma^{A,\beta}_{(1,2,3,4),\mu}]\\&=\int\left(\frac{dx_1d^2\vec{k}_{1\perp}}{2(2\pi)^3}\right)\left(\frac{dx_2d^2\vec{k}_{2\perp}}{2(2\pi)^3}\right)\frac{\psi_b(x_i,\vec{k}_{i\perp})\psi_s^*(x_i',\vec{k}_{i\perp}')}{\sqrt{x_3x_3'}}A_0B_0'\\&\quad\times\mathrm{Tr}[\cdots]\mathrm{Tr}[(G_{G_{\Lambda^*}})_{\beta\alpha}K'^{\alpha}(\not{p}_3'+m_3')\gamma^\mu\gamma^5(\not{p}_3+m_3)(\not{P}+M_0)\Gamma^{A,\beta}_{(1,2,3,4),\mu}],\end{aligned}\tag{3.17}$$

$$\begin{aligned}&\mathrm{Tr}[(G_{\Lambda^*})^{\beta\alpha}.[\text{form factors in Eq.(2.9)}].(\not{P}+M_0).\Gamma^{T,\beta}_{(1,2,3),\mu}]\\&=\int\left(\frac{dx_1d^2\vec{k}_{1\perp}}{2(2\pi)^3}\right)\left(\frac{dx_2d^2\vec{k}_{2\perp}}{2(2\pi)^3}\right)\frac{\psi_b(x_i,\quad\vec{k}_{i\perp})\psi_s^*(x_i',\vec{k}_{i\perp}')}{\sqrt{x_3x_3'}}A_0B_0'\mathrm{Tr}[\cdots]\\&\quad\times\mathrm{Tr}[(G_{G_{\Lambda^*}})_{\beta\alpha}K'^{\alpha}(\not{p}_3'+m_3')i\sigma^{\mu\nu}q_\nu(\not{p}_3+m_3)(\not{P}+M_0)\Gamma^{T,\beta}_{(1,2,3),\mu}],\end{aligned}\tag{3.18}$$

$$\begin{aligned}&\mathrm{Tr}[(G_{\Lambda^*})^{\beta\alpha}.[\text{form factors in Eq.(2.10)}].(\not{P}+M_0).\Gamma^{T5,\beta}_{(1,2,3),\mu}]\\&=\int\left(\frac{dx_1d^2\vec{k}_{1\perp}}{2(2\pi)^3}\right)\left(\frac{dx_2d^2\vec{k}_{2\perp}}{2(2\pi)^3}\right)\frac{\psi_b(x_i,\vec{k}_{i\perp})\psi_s^*(x_i',\vec{k}_{i\perp}')}{\sqrt{x_3x_3'}}A_0B_0'\mathrm{Tr}[\cdots]\\&\quad\times\mathrm{Tr}[(G_{G_{\Lambda^*}})_{\beta\alpha}K'^{\alpha}(\not{p}_3'+m_3')i\sigma^{\mu\nu}q_\nu\gamma^5(\not{p}_3+m_3)(\not{P}+M_0)\Gamma^{T5,\beta}_{(1,2,3),\mu}].\end{aligned}\tag{3.19}$$

This approach has been used to evaluate the form factors of triple heavy baryon transitions from $3/2\to1/2$ cases [71,72].

IV. THE SEMIRELATIVISTIC POTENTIAL MODEL FOR CALCULATING BARYON WAVE FUNCTION

In this section, we will derive the wave function using the GEM with semirelativistic potential model. In general, to obtain the wave function and mass of a baryon, we need to solve the three-body Schrödinger equation,

$$\mathcal{H}\Psi_{\mathbf{J},\mathbf{M_J}}=E\Psi_{\mathbf{J},\mathbf{M_J}},\tag{4.1}$$

where $\mathcal{H}$ is the Hamiltonian and E is the corresponding eigenvalue. It can be solved by using the Rayleigh-Ritz variational principle.

Unlike a meson system, a baryon in the traditional quark model is a typical three-body system. In our calculation, the semirelativistic potentials used in Refs. [73–75] are applied. The Hamiltonian in question [73,74],

$$\mathcal{H}=K+\sum_{i<j}(S_{ij}+G_{ij}+V_{ij}^{\mathrm{so(s)}}+V_{ij}^{\mathrm{so(v)}}+V_{ij}^{\mathrm{ten}}+V_{ij}^{\mathrm{con}}),\tag{4.2}$$

includes the kinetic energy K, the spin-independent linear confinement piece S, the Coulomb-like potential G, and the higher-order terms containing the scalar-type spin-orbit interaction $V^{\mathrm{so}(s)}$, the vector-type spin-orbit interaction $V^{\mathrm{so}(v)}$, the tensor potential V^{tens}, and the spin-dependent contact potential V^{con}. The concrete expressions are given as [73–75]

$$K=\sum_{i=1,2,3}\sqrt{m_i^2+p_i^2},\tag{4.3}$$

$$S_{ij}=-\frac{3}{4}\left(br_{ij}\left[\frac{e^{-\sigma^2r_{ij}^2}}{\sqrt{\pi}\sigma r_{ij}}+\left(1+\frac{1}{2\sigma^2r_{ij}^2}\right)\frac{2}{\sqrt{\pi}}\times\int_0^{\sigma r_{ij}}e^{-x^2}dx\right]\right)\mathbf{F_i}\cdot\mathbf{F_j}+\frac{c}{3},\tag{4.4}$$

$$G_{ij}=\sum_k\frac{\alpha_k}{r_{ij}}\left[\frac{2}{\sqrt{\pi}}\int_0^{\tau_kr_{ij}}e^{-x^2}dx\right]\mathbf{F_i}\cdot\mathbf{F_j}\tag{4.5}$$

for the spin-independent terms with

$$\sigma^2=\sigma_0^2\left[\frac{1}{2}+\frac{1}{2}\left(\frac{4m_im_j}{(m_i+m_j)^2}\right)^4+s^2\left(\frac{2m_im_j}{m_i+m_j}\right)^2\right],\tag{4.6}$$

and the $\langle\mathbf{F_i}\cdot\mathbf{F_j}\rangle=-2/3$ for the quark-quark interaction, and

$$V_{ij}^{\mathrm{so}(s)}=-\frac{\mathbf{r_{ij}}\times\mathbf{p_i}\cdot\mathbf{S_i}}{2m_i^2}\frac{1}{r_{ij}}\frac{\partial S_{ij}}{\partial r_{ij}}+\frac{\mathbf{r_{ij}}\times\mathbf{p_j}\cdot\mathbf{S_j}}{2m_j^2}\frac{1}{r_{ij}}\frac{\partial S_{ij}}{\partial r_{ij}},\tag{4.7}$$

$$\begin{aligned}V_{ij}^{\mathrm{so}(v)}=&\frac{\mathbf{r_{ij}}\times\mathbf{p_i}\cdot\mathbf{S_i}}{2m_i^2}\frac{1}{r_{ij}}\frac{\partial G_{ij}}{\partial r_{ij}}-\frac{\mathbf{r_{ij}}\times\mathbf{p_j}\cdot\mathbf{S_j}}{2m_j^2}\frac{1}{r_{ij}}\frac{\partial G_{ij}}{\partial r_{ij}}\\&-\frac{\mathbf{r_{ij}}\times\mathbf{p_j}\cdot\mathbf{S_i}-\mathbf{r_{ij}}\times\mathbf{p_i}\cdot\mathbf{S_j}}{m_im_j}\frac{1}{r_{ij}}\frac{\partial G_{ij}}{\partial r_{ij}},\end{aligned}\tag{4.8}$$

$$\begin{aligned}V_{ij}^{\mathrm{tens}}=&-\frac{1}{m_im_j}\left[(\mathbf{S_i}\cdot\hat{\mathbf{r}}_{\mathbf{ij}})(\mathbf{S_j}\cdot\hat{\mathbf{r}}_{\mathbf{ij}})-\frac{\mathbf{S_i}\cdot\mathbf{S_j}}{3}\right]\\&\times\left(\frac{\partial^2G_{ij}}{\partial r_{ij}^2}-\frac{\partial G_{ij}}{r_{ij}\partial r_{ij}}\right),\end{aligned}\tag{4.9}$$

$$V_{ij}^{\mathrm{con}}=\frac{2\mathbf{S_i}\cdot\mathbf{S_j}}{3m_im_j}\nabla^2G_{ij}\tag{4.10}$$

TABLE I. The parameters used in the semirelativistic potential model. The quark masses are also chosen to be $m_u = 220$ MeV, $m_d = 220$ MeV, $m_s = 419$ MeV, $m_c = 1628$ MeV, and $m_b = 4977$ MeV [75,76].

Parameters	Values	Parameters	Values
b (GeV^2)	0.1466 ± 0.0007	$\epsilon^{so(s)}$	0.5000 ± 0.0762
c (GeV)	-0.3490 ± 0.0050	$\epsilon^{so(v)}$	-0.1637 ± 0.0131
σ_0 (GeV)	1.7197 ± 0.0304	ϵ^{tens}	-0.3790 ± 0.5011
s	0.5278 ± 0.0718	ϵ^{con}	-0.1612 ± 0.0015

for the spin-dependent terms, where m_i is the mass of the ith constituent quark, and $\mathbf{S_i}$ is the corresponding spin operator.

Next, a general transformation based on the center of mass of the interacting quarks and the momentum is set up to compensate for the loss of relativistic effect in the nonrelativistic limit [75,76]

$$G_{ij} \to \left(1+\frac{p^2}{E_iE_j}\right)^{1/2} G_{ij} \left(1+\frac{p^2}{E_iE_j}\right)^{1/2},$$
$$\frac{V^k_{ij}}{m_im_j} \to \left(\frac{m_im_j}{E_iE_j}\right)^{1/2+\epsilon_k} \frac{V^k_{ij}}{m_im_j} \left(\frac{m_im_j}{E_iE_j}\right)^{1/2+\epsilon_k}, \quad (4.11)$$

where $E_i = \sqrt{p^2+m_i^2}$ is the energy of the ith constituent quark, the subscript k is used to distinguish the contact, tensor, vector spin-orbit, and scalar spin-orbit terms, and the ϵ_k is used to denote the relevant modification parameters, which are collected in Table I.

The total wave function of the baryon is composed of color, spin, spatial, and flavor wave functions, i.e.,

$$\Psi_{\mathbf{J},\mathbf{M_J}} = \chi^{\text{color}} \{\chi^{\text{spin}}{}_{\mathbf{S},\mathbf{M_S}} \psi^{\text{spatial}}_{\mathbf{L},\mathbf{M_L}}(\vec{\rho},\vec{\lambda})\}_{\mathbf{J},\mathbf{M_J}} \psi^{\text{flavor}}, \quad (4.12)$$

where $\chi^{\text{color}} = (rgb - rbg + gbr - grb + brg - bgr)/\sqrt{6}$ is the universal color wave function for the baryon. For the affected Λ_b and Λ^*, their flavor wave functions are chosen as $\psi^{\text{flavor}} = (ud - du)Q/\sqrt{2}$ where $Q = b$ or s. Also, $\mathbf{S}$ is the total spin and $\mathbf{L}$ is the total orbital angular momentum. $\psi^{\text{spatial}}_{\mathbf{L},\mathbf{M_L}}$ is the spatial wave function, which is composed of the ρ mode and λ mode

$$\psi^{\text{partial}}_{\mathbf{L},\mathbf{M_L}}(\vec{\rho},\vec{\lambda}) = \{\phi_{\boldsymbol{l_\rho},\boldsymbol{ml_\rho}}(\vec{\rho})\phi_{\boldsymbol{l_\lambda},\boldsymbol{ml_\lambda}}(\vec{\lambda})\}_{\mathbf{L},\mathbf{M_L}}, \quad (4.13)$$

where the subscripts $\boldsymbol{l_\rho}$ and $\boldsymbol{l_\lambda}$ represent the orbital angular momentum quanta for the ρ and λ modes, respectively, and the internal Jacobi coordinates are chosen to be

$$\vec{\rho} = \vec{r}_2 - \vec{r}_1,$$
$$\vec{\lambda} = \vec{r}_3 - \frac{m_1\vec{r}_1 + m_2\vec{r}_2}{m_1+m_2}. \quad (4.14)$$

As shown in Fig. 1, the $\Lambda_b(\Lambda^*)$ is considered as a bound state with the u and d quarks bound to form the ρ mode and then bounded to the b (or s) quark to form the λ mode.

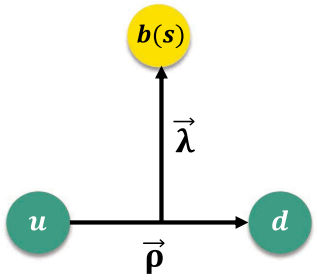

FIG. 1. The definition of the internal Jacobi coordinates $\vec{\rho}$ and $\vec{\lambda}$, where we use green spheres to represent the u and d quarks and yellow spheres to represent the b (or s) quark.

In this calculation, the Gaussian basis [44–46],

$$\phi^G_{nlm}(\vec{r}) = \phi^G_{nl}(r)Y_{lm}(\hat{r}) = \sqrt{\frac{2^{l+2}(2\nu_n)^{l+3/2}}{\sqrt{\pi}(2l+1)!!}} \lim_{\varepsilon\to 0} \frac{1}{(\nu_n\varepsilon)^l} \sum_{k=1}^{k_{\max}} C_{lm,k} e^{-\nu_n(\vec{r}-\varepsilon\vec{D}_{lm,k})^2}, \quad (4.15)$$

is used to expand the spatial wave functions $\phi_{\boldsymbol{l_\rho},\boldsymbol{ml_\rho}}$ and $\phi_{\boldsymbol{l_\lambda},\boldsymbol{ml_\lambda}}$ $(n = 1, 2, \ldots, n_{\max})$, where the freedom parameter $n_{\max}$ should be chosen from positive integers, and then the Gaussian size parameter ν_n can be settled as [77]

$$\nu_n = 1/r_n^2, \qquad r_n = r_{\min}a^{n-1}, \quad (4.16)$$

where

$$a = \left(\frac{r_{\max}}{r_{\min}}\right)^{\frac{1}{n_{\max}-1}}.$$

In our calculation the values of $\rho_{\min}$ and $\rho_{\max}$ are chosen to be 0.2 fm and 2.0 fm, respectively, and the parameter $n_{\rho_{\max}} = 6$. For the λ mode, we also use the same Gaussian-sized parameters.

In this paper, we fit the single charmed and bottom baryon spectrum to fix the phenomenological parameters in the semirelativistic potential model. The experimentally observed masses of charmed and bottom baryons are collected in Table II. The χ^2 method, i.e., finding the minimum χ^2 value, is used for the fitting. In our fit, the χ^2 value is defined as

$$\chi^2 = \frac{1}{n(n-1)} \sum_i^n \left(\frac{m_i^{\text{Exp}} - m_i^{\text{The}}}{\sigma_i}\right)^2, \quad (4.17)$$

where m_i^{Exp} and m_i^{The} are experimental and theoretical values of the mass of the ith baryon, respectively. The errors $\sigma_i = 1$ MeV[1] are universal for all baryons. In this fitting, the χ^2 is given as 2.84. The fitted parameters are collected in

[1]Checking the PDG [58], we find that the uncertainties of the measured masses of the charmed and bottom baryons are around a few MeV. In order to make the baryons act in the same proportions in our fitting, we choose a universe value of 1 MeV as the uncertainty.

TABLE II. Experimentally observed masses of charmed and bottom baryons used to fit the potential model parameters, where only the central values are given.

States	J^P	This work (GeV)	Experiment (GeV) [58]	States	J^P	This work (GeV)	Experiment (GeV) [58]
Λ_c	$\frac{1}{2}^+$	2.286	2.286	Λ_b	$\frac{1}{2}^+$	5.621	5.619
$\Lambda_c(2595)$	$\frac{1}{2}^-$	2.595	2.595	$\Lambda_b(5912)$	$\frac{1}{2}^-$	5.896	5.912
$\Lambda_c(2625)$	$\frac{3}{2}^-$	2.627	2.625	$\Lambda_b(5920)$	$\frac{3}{2}^-$	5.909	5.919
$\Lambda_c(2765)$	$?^?$	2.768	2.765	$\Lambda_b(6070)$	$\frac{1}{2}^+$	6.046	6.072
$\Lambda_c(2860)$	$\frac{3}{2}^+$	2.872	2.856	$\Lambda_b(6146)$	$\frac{3}{2}^+$	6.133	6.146
$\Lambda_c(2880)$	$\frac{5}{2}^+$	2.894	2.881	$\Lambda_b(6152)$	$\frac{5}{2}^+$	6.144	6.152
Σ_c	$\frac{1}{2}^+$	2.446	2.453	Σ_b	$\frac{1}{2}^+$	5.809	5.811
$\Sigma_c(2520)$	$\frac{3}{2}^+$	2.519	2.518	Σ_b^*	$\frac{3}{2}^+$	5.835	5.832
Ξ_c	$\frac{1}{2}^+$	2.478	2.467	Ξ_b	$\frac{1}{2}^+$	5.809	5.794
$\Xi_c(2790)$	$\frac{1}{2}^-$	2.787	2.792	$\Xi_b(6100)$	$\frac{3}{2}^-$	6.093	6.100
$\Xi_c(2815)$	$\frac{3}{2}^-$	2.814	2.816	$\Xi_b(6327)$ [78]	$?^?$	6.316	6.327
$\Xi_c(2970)$	$?^?$	2.953	2.970	$\Xi_b(6333)$ [78]	$?^?$	6.324	6.332
$\Xi_c(3055)$	$?^?$	3.059	3.055	$\Xi_b'(5935)$	$\frac{1}{2}^+$	5.939	5.935
$\Xi_c(3080)$	$?^?$	3.077	3.080	$\Xi_b(5945)$	$\frac{3}{2}^+$	5.963	5.949
Ξ_c'	$\frac{1}{2}^+$	2.583	2.577	Ω_b	$\frac{1}{2}^+$	6.043	6.046
$\Xi_c(2645)$	$\frac{3}{2}^+$	2.648	2.645				
Ω_c	$\frac{1}{2}^+$	2.693	2.695				
$\Omega_c(2770)$	$\frac{3}{2}^+$	2.755	2.765				

Table I. Meanwhile, our results for the masses of the charmed and bottom baryons are presented in Table II.

With the above preparations, we can calculate the spatial wave functions of Λ_b and $\Lambda(1520)$. Their masses and radial components of spatial wave functions are shown in Table III. It is obvious that the calculated mass of Λ_b is consistent with the Particle Data Group (PDG) [58] averaged value, while that of $\Lambda(1520)$ is about 40 MeV higher than the PDG value.

V. NUMERICAL RESULTS

A. The weak transition form factors

With the input of the numerical wave functions of Λ_b and Λ^*, and the complete expressions of the form factors obtained by solving Eq. (3.12) and Eqs. (3.17)–(3.19), we present our numerical results of the form factors of the $\Lambda_b \to \Lambda^*$ transition. Since the form factors calculated in the light-front quark model are valid in the spacelike region ($q^2 < 0$), we have to extrapolate them to the timelike region ($q^2 > 0$).

Before we do the extrapolation, we need to talk about some constraints on the form factors at the $q^2 = q^2_{\rm max}$ point. To make sure that the helicity amplitudes in Eqs. (2.22)–(2.25) have no singularities and are nonzero values in the $q^2 \to q^2_{\rm max}$ limit, we get the constraints in this limit as

$$
\begin{aligned}
&f_t^V = O\left(\frac{1}{\sqrt{s_-}}\right), \quad f_0^V = O\left(\frac{1}{s_-}\right), \quad f_\perp^V = O\left(\frac{1}{s_-}\right), \quad f_g^V = O(1),\\
&f_t^A = O\left(\frac{1}{s_-}\right), \quad f_0^A = O\left(\frac{1}{\sqrt{s_-}}\right), \quad f_\perp^A = O\left(\frac{1}{\sqrt{s_-}}\right), \quad f_g^A = O\left(\frac{1}{\sqrt{s_-}}\right),\\
&f_0^T = O\left(\frac{1}{s_-}\right), \quad f_\perp^T = O\left(\frac{1}{s_-}\right), \quad f_g^T = O(1),\\
&f_0^{T5} = O\left(\frac{1}{\sqrt{s_-}}\right), \quad f_\perp^{T5} = O\left(\frac{1}{\sqrt{s_-}}\right), \quad f_g^{T5} = O\left(\frac{1}{\sqrt{s_-}}\right).0
\end{aligned}
\tag{5.1}
$$

TABLE III. The comparison of the masses of Λ_b and $\Lambda(1520)$ from our calculation and the PDG [58] data, and the radial components of the spatial wave functions of the concerned Λ_b and $\Lambda(1520)$ from the semirelativistic potential model and GEM. The Gaussian bases (n_ρ, n_λ) listed in the fourth column are arranged as $[(1,1),(1,2),\ldots,(1,n_{\lambda_{\max}}),(2,1),(2,2),\ldots,(2,n_{\lambda_{\max}}),\ldots,(n_{\rho_{\max}},1),(n_{\rho_{\max}},2),\ldots,(n_{\rho_{\max}},n_{\lambda_{\max}})]$.

States	This work (GeV)	Experiment (MeV) [58]	Eigenvectors
Λ_b	5.621 ± 0.005	5619.60 ± 0.17	$[0.0068 \pm 0.0007, 0.0442 \pm 0.0014, 0.0732 \pm 0.0016, 0.0032 \pm 0.0003,$ $0.0011 \pm 0.0001, -0.0004 \pm 0.0000, 0.0270 \pm 0.0012, 0.0204 \pm 0.0010,$ $0.0273 \pm 0.0022, 0.0067 \pm 0.0004, -0.0027 \pm 0.0001, 0.0007 \pm 0.0000,$ $-0.0170 \pm 0.0002, 0.2541 \pm 0.0058, 0.2427 \pm 0.0006, 0.0005 \pm 0.0002,$ $0.0060 \pm 0.0001, -0.0017 \pm 0.0000, -0.0037 \pm 0.0003, -0.0426 \pm 0.0010,$ $0.4052 \pm 0.0028, 0.0253 \pm 0.0025, -0.0023 \pm 0.0007, 0.0004 \pm 0.0002,$ $0.0071 \pm 0.0001, -0.0052 \pm 0.0008, 0.0105 \pm 0.0008, 0.1224 \pm 0.0015,$ $-0.0246 \pm 0.0001, 0.0054 \pm 0.0000, -0.0020 \pm 0.0000, 0.0010 \pm 0.0003,$ $-0.0112 \pm 0.0003, -0.0139 \pm 0.0001, 0.0086 \pm 0.0001, -0.0017 \pm 0.0000]$
$\Lambda(1520)$	1.561 ± 0.007	1517.5 ± 0.4	$[0.0000 \pm 0.0001, -0.0096 \pm 0.0004, -0.0488 \pm 0.0017, -0.0576 \pm 0.0010$ $-0.0011 \pm 0.0001, -0.0004 \pm 0.0000, -0.0049 \pm 0.0004, 0.0041 \pm 0.0002$ $-0.0295 \pm 0.0012, -0.0279 \pm 0.0020, 0.0011 \pm 0.0003, -0.0006 \pm 0.0002$ $-0.0010 \pm 0.0001, -0.0510 \pm 0.0019, -0.1771 \pm 0.0036, -0.1890 \pm 0.0014$ $-0.0036 \pm 0.0004, -0.0008 \pm 0.0003, 0.0003 \pm 0.0001, 0.0222 \pm 0.0005$ $-0.2146 \pm 0.0003, -0.2766 \pm 0.0040, -0.0001 \pm 0.0013, -0.0036 \pm 0.0006$ $-0.0025 \pm 0.0001, 0.0028 \pm 0.0001, 0.0135 \pm 0.0012, -0.1653 \pm 0.0011$ $-0.0174 \pm 0.0008, 0.0019 \pm 0.0005, 0.0010 \pm 0.0000, -0.0020 \pm 0.0000$ $0.0035 \pm 0.0004, 0.0277 \pm 0.0002, -0.0061 \pm 0.0005, 0.0010 \pm 0.0003]$

The form factors that show less singular behavior in the $q^2 \to q^2_{\max}$ limit are also reasonable. This would lead the helicity amplitudes to be zero in $q^2 = q^2_{\max}$. The above features have been discussed in Ref. [31]. However, the above requirement is not strict enough, since it gives a broad limit. This will make nonunique extrapolations of the form factors.

Since the LQCD calculation of $\Lambda_b \to \Lambda(1520)$ form factors has been done in Refs. [28,29], and their results work well in the kinematic region near $q^2_{\max}$, we will talk about the characters of the form factors in the LQCD. The LQCD calculation has been completed in Refs. [28,29]. The authors obtained finite values of the form factors of $\Lambda_b \to \Lambda(1520)$ in their definition (i.e., $f_{0,+,\perp,\perp'}$, $g_{0,+,\perp,\perp'}$, $h_{+,\perp,\perp'}$, and $\tilde{h}_{+,\perp,\perp'}$) in the $q^2 = q^2_{\max}$ limit. Their definition of the form factors can be converted to ours by [28]

$$
\begin{aligned}
&f_t^V = \frac{m_{\Lambda^*}}{s_+} f_0, \quad f_0^V = \frac{m_{\Lambda^*}}{s_-} f_+, \quad f_\perp^V = \frac{m_{\Lambda^*}}{s_-} f_\perp, \quad f_g^V = f_{\perp'},\\
&f_t^A = \frac{m_{\Lambda^*}}{s_-} g_0, \quad f_0^A = \frac{m_{\Lambda^*}}{s_+} g_+, \quad f_\perp^A = \frac{m_{\Lambda^*}}{s_+} g_\perp, \quad f_g^A = -g_{\perp'},\\
&f_0^T = \frac{m_{\Lambda^*}}{s_-} h_+, \quad f_\perp^T = \frac{m_{\Lambda^*}}{s_-} h_\perp, \quad f_g^T = (m_{\Lambda_b} + m_{\Lambda^*}) h_{\perp'},\\
&f_0^{T5} = \frac{m_{\Lambda^*}}{s_+} \tilde{h}_+, \quad f_\perp^{T5} = \frac{m_{\Lambda^*}}{s_+} \tilde{h}_\perp, \quad f_g^{T5} = -(m_{\Lambda_b} - m_{\Lambda^*}) \tilde{h}_{\perp'}.
\end{aligned}
\tag{5.2}
$$

This shows that in the $q^2 = q^2_{\max}$ limit, the LQCD results [29] show

$$
\begin{aligned}
&f_t^V = O(1), \quad f_0^V = O\left(\frac{1}{s_-}\right), \quad f_\perp^V = O\left(\frac{1}{s_-}\right), \quad f_g^V = O(1),\\
&f_0^A = O(1), \quad f_\perp^A = O(1), \quad f_g^A = O(1),\\
&f_0^T = O\left(\frac{1}{s_-}\right), \quad f_\perp^T = O\left(\frac{1}{s_-}\right), \quad f_g^T = O(1),\\
&f_0^{T5} = O(1), \quad f_\perp^{T5} = O(1), \quad f_g^{T5} = O(1).
\end{aligned}
\tag{5.3}
$$

These characters fulfill the requirements. Also we have $g_0(q^2) = \frac{a_1^{g_0}}{1-q^2/(m_{\text{pole}}^f)^2}(\omega - 1)$ [29] with $\omega = (m^2_{\Lambda_b} + m^2_{\Lambda^*} - q^2)/(2m_{\Lambda_b} m_{\Lambda^*})$, where $a_1^{g_0}$ is a nonzero value. According to Eq. (5.2), the $f_t^A(q^2) = \frac{m_{\Lambda^*}}{s_-} \frac{a_1^{g_0}}{1-q^2/(m_{\text{pole}}^f)^2}(\omega - 1)$, and this implies, in the $q^2 = q^2_{\max}$ limit, that $f_t^A = O(1)$. This also satisfies the requirement.

In order to align with the LQCD results, we take the following strategy for the analytical continuation:

(1) To do the extrapolations of the form factors $f^V_{t,g}$, $f^A_{t,0,\perp,g}$, f^T_g, and $f^{T5}_{0,\perp,g}$, the z-series form [34,79–81]

$$
f(q^2) = \frac{1}{1 - q^2/(m_{\text{pole}}^f)^2} \times \left[a_0^f + a_1^f z^f(q^2) + a_2^f (z^f(q^2))^2\right] \tag{5.4}
$$

is adopted where a_0^f, a_1^f, and a_2^f are free parameters needed to fit in the spacelike region, and

TABLE IV. The pole masses of the form factors in Eq. (5.4), where the 0^-, 1^-, and 1^+ masses are taken from the PDG [58], while the 0^+ mass is taken from the LQCD calculation [82].

f	J^P	$m^f_{\rm pole}$ (GeV)
f_t^V	0^+	5.711
f_g^V, f_g^T	1^-	5.415
f_t^A	0^-	5.367
f_0^A, $f_\perp^A$, f_g^A, f_0^{T5}, $f_\perp^{T5}$, f_g^{T5}	1^+	5.828

$$z^f(q^2)=\frac{\sqrt{t_+^f-q^2}-\sqrt{t_+^f-t_0}}{\sqrt{t_+^f-q^2}+\sqrt{t_+^f-t_0}},$$
$$t_\pm^f=(m_B\pm m_K)^2. \tag{5.5}$$

The parameter t_0 is set to

$$0\le t_0=t_+\left(1-\sqrt{1-\frac{t_-}{t_+}}\right)\le t_-. \tag{5.6}$$

The $m^f_{\rm pole}$ is collected in Table IV.

(2) For the form factors $f^V_{0,\perp}$ and $f^T_{0,\perp}$, we use the form as

$$f(q^2)=\frac{1}{1-q^2/m_-^2}\left[a_0^f+a_1^f z^f(q^2)+a_2^f(z^f(q^2))^2\right], \tag{5.7}$$

where $m_-=m_{\Lambda_b}-m_{\Lambda^*}$.

To determine the parameters a_0^f, a_1^f, and a_2^f, we numerically calculate 24 points for each form factor by Eqs. (3.12)–(3.19) from $q^2=-q^2_{\rm max}$ to $q^2=-0.01$ GeV^2 in the spacelike region, and then fit them using Eqs. (5.4) and (5.7) with the MINUIT program. The extrapolated parameters for the form factors of $\Lambda_b\to\Lambda^*$ are collected in Table V. The q^2 dependence of the concerned form factors is shown in Fig. 2.

However, as discussed earlier, the less singular behaviors of $f^V_{0,\perp}$ and $f^T_{0,\perp}$ in the small-recoil limit are also not forbidden. Therefore, in this work, we also use the formula in Eq. (5.4) to perform the extrapolation of the form factors $f^V_{0,\perp}$ and $f^T_{0,\perp}$ again. This extrapolation scheme gives different results at the $q^2=q^2_{\rm max}$ point for the four form factors, but has no effect on other form factors compared with the previous scheme. For clarification, we compare our results of the form factors in the $q^2=q^2_{\rm max}$ point with the two different extrapolation schemes in Table VI. Finally, it should be emphasized that there is no established procedure for the extrapolation. The experimental measurement of $\Lambda_b\to\Lambda(1520)\ell^+\ell^-$ by the LHCb Collaboration can test the different extrapolation schemes.

As shown in Eqs. (2.7)–(2.10), we need eight (axial-)vector and six (pseudo-)tensor form factors to describe the matrix elements in question. The number can apparently be reduced in the heavy quark limit $m_b\to\infty$. We speak separately of two different kinematic situations, i.e., the outgoing Λ^* acts softly (the low-recoil limit) and acts energetically (the large-recoil limit). Accordingly, two effective theories, namely heavy quark effective theory (HQET) and soft-collinear effective theory (SCET), are developed to exploit the behaviors of the form factors.

TABLE V. The form factors of the $\Lambda_b\to\Lambda^*$ transition in the standard light-front quark model.

Parameter	Value	Parameter	Value	Parameter	Value
$a_0^{f_t^V}$	(0.1041 ± 0.0036) GeV^{-1}	$a_1^{f_t^V}$	(-0.4493 ± 0.0375) GeV^{-1}	$a_2^{f_t^V}$	(0.5425 ± 0.0954) GeV^{-1}
$a_0^{f_0^V}$	(0.0850 ± 0.0037) GeV^{-1}	$a_1^{f_0^V}$	(-0.2465 ± 0.0386) GeV^{-1}	$a_2^{f_0^V}$	(0.0637 ± 0.0984) GeV^{-1}
$a_0^{f_\perp^V}$	(0.1538 ± 0.0046) GeV^{-1}	$a_1^{f_\perp^V}$	(-0.7505 ± 0.0478) GeV^{-1}	$a_2^{f_\perp^V}$	(1.0292 ± 0.1210) GeV^{-1}
$a_0^{f_g^V}$	0.0223 ± 0.0001	$a_1^{f_g^V}$	-0.0807 ± 0.0003	$a_2^{f_g^V}$	0.0798 ± 0.0031
$a_0^{f_t^A}$	(0.1052 ± 0.0026) GeV^{-1}	$a_1^{f_t^A}$	(-0.5337 ± 0.0263) GeV^{-1}	$a_2^{f_t^A}$	(0.7542 ± 0.0665) GeV^{-1}
$a_0^{f_0^A}$	(0.0878 ± 0.0028) GeV^{-1}	$a_1^{f_0^A}$	(-0.3647 ± 0.0293) GeV^{-1}	$a_2^{f_0^A}$	(0.4197 ± 0.0747) GeV^{-1}
$a_0^{f_\perp^A}$	(0.0804 ± 0.0022) GeV^{-1}	$a_1^{f_\perp^A}$	(-0.3619 ± 0.0227) GeV^{-1}	$a_2^{f_\perp^A}$	(0.4573 ± 0.0578) GeV^{-1}
$a_0^{f_g^A}$	0.0441 ± 0.0023	$a_1^{f_g^A}$	-0.2012 ± 0.0240	$a_2^{f_g^A}$	0.2596 ± 0.0605
$a_0^{f_0^T}$	(-0.0178 ± 0.0003) GeV^{-1}	$a_1^{f_0^T}$	(0.5398 ± 0.0037) GeV^{-1}	$a_2^{f_0^T}$	(-1.4719 ± 0.0098) GeV^{-1}
$a_0^{f_\perp^T}$	(0.0565 ± 0.0032) GeV^{-1}	$a_1^{f_\perp^T}$	(-0.0233 ± 0.0331) GeV^{-1}	$a_2^{f_\perp^T}$	(-0.3596 ± 0.0853) GeV^{-1}
$a_0^{f_g^T}$	(0.0851 ± 0.0034) GeV	$a_1^{f_g^T}$	(-0.4603 ± 0.0334) GeV	$a_2^{f_g^T}$	(0.6616 ± 0.0805) GeV
$a_0^{f_0^{T5}}$	(0.0923 ± 0.0026) GeV^{-1}	$a_1^{f_0^{T5}}$	(-0.4516 ± 0.0272) GeV^{-1}	$a_2^{f_0^{T5}}$	(0.6337 ± 0.0687) GeV^{-1}
$a_0^{f_\perp^{T5}}$	(0.0790 ± 0.0020) GeV^{-1}	$a_1^{f_\perp^{T5}}$	(-0.3482 ± 0.0206) GeV^{-1}	$a_2^{f_\perp^{T5}}$	(0.4288 ± 0.0527) GeV^{-1}
$a_0^{f_g^{T5}}$	(-0.3839 ± 0.0276) GeV	$a_1^{f_g^{T5}}$	(1.6524 ± 0.2814) GeV	$a_2^{f_g^{T5}}$	(-2.1223 ± 0.6945) GeV

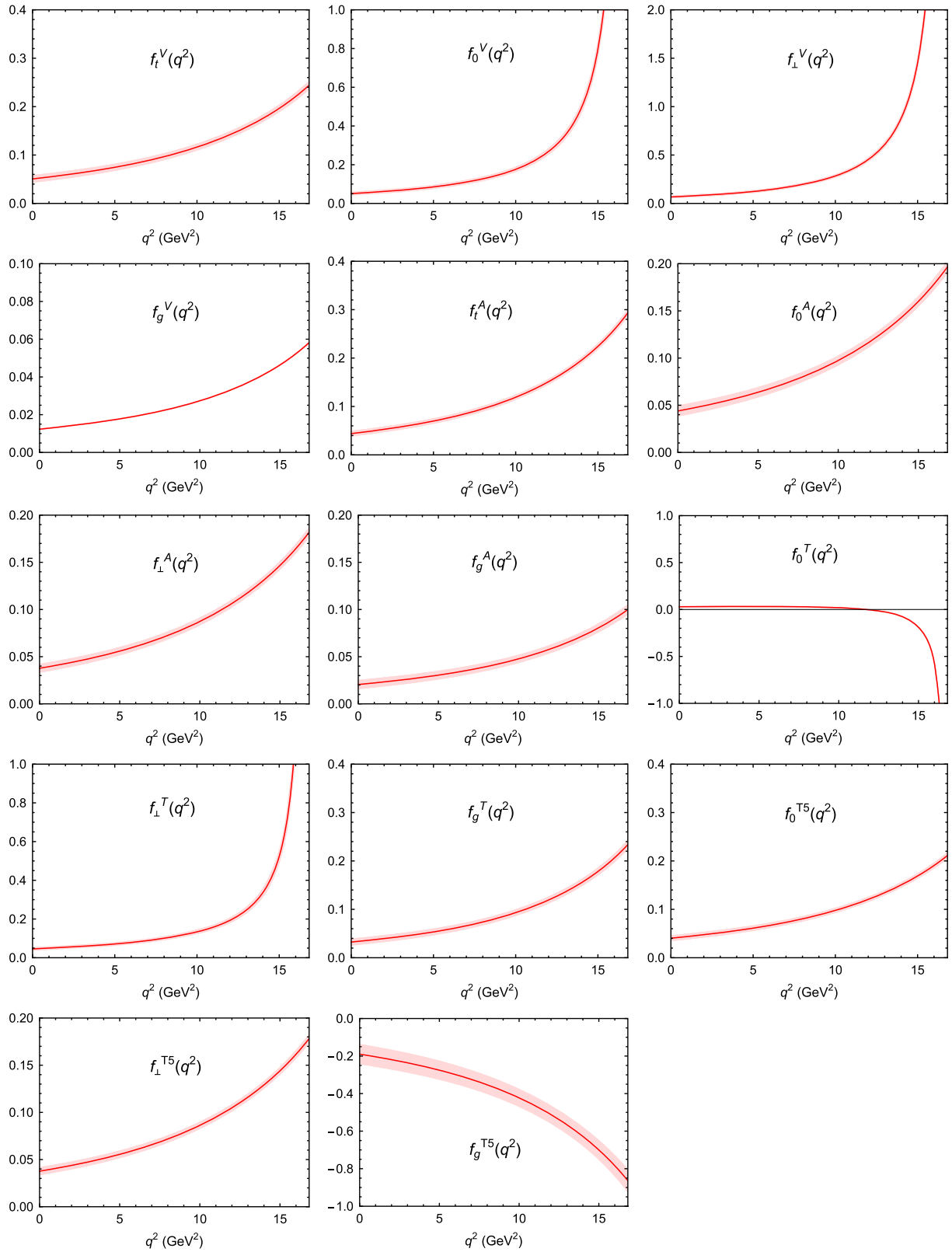

FIG. 2. The q^2 dependence of the form factors of the vector, axial-vector, tensor, and pseudotensor type currents of the $\Lambda_b \to \Lambda^*$ transition, where the red solid curves are central values, and the light red bands are the corresponding errors. The units of the form factors are neglected here.

TABLE VI. Theoretical predictions for the form factors of $\Lambda_b \to \Lambda(1520)$ at the endpoints of $q^2 = 0$ and $q^2 = q^2_{\rm max}$ using different approaches.

	This work	NRQM [22]	LQCD [29]		This work [a]	This work [b]	NRQM [22]	LQCD [29]
$f_t^V(0)$	0.051 ± 0.007	0.0029	-0.1523 ± 0.0530	$f_t^V(q^2_{\rm max})$	0.244 ± 0.008	0.244 ± 0.008	∞	0.1726 ± 0.0138
$f_0^V(0)$	0.051 ± 0.007	0.0029	0.0714 ± 0.0078	$f_0^V(q^2_{\rm max})$	∞	0.336 ± 0.008	∞	∞
$f_\perp^V(0)$	0.067 ± 0.009	0.0042	0.1093 ± 0.0151	$f_\perp^V(q^2_{\rm max})$	∞	0.416 ± 0.011	∞	∞
$f_g^V(0)$	0.0123 ± 0.0001	-0.0002	-0.0385 ± 0.0138	$f_g^V(q^2_{\rm max})$	0.0582 ± 0.0002	0.0582 ± 0.0002	0.0323	0.0481 ± 0.0028
$f_t^A(0)$	0.044 ± 0.005	0.0031	0.0705 ± 0.0060	$f_t^A(q^2_{\rm max})$	0.293 ± 0.006	0.293 ± 0.006	∞	0.1695 ± 0.0145
$f_0^A(0)$	0.044 ± 0.005	0.0031	-0.1283 ± 0.0471	$f_0^A(q^2_{\rm max})$	0.197 ± 0.006	0.197 ± 0.006	0.1791	0.1449 ± 0.0109
$f_\perp^A(0)$	0.038 ± 0.004	0.0033	-0.1260 ± 0.0471	$f_\perp^A(q^2_{\rm max})$	0.182 ± 0.005	0.182 ± 0.005	0.1637	0.1430 ± 0.0109
$f_g^A(0)$	0.020 ± 0.004	0.0004	0.0086 ± 0.0830	$f_g^A(q^2_{\rm max})$	0.100 ± 0.005	0.100 ± 0.005	0.0532	0.0415 ± 0.0145
$f_0^T(0)$	0.0294 ± 0.0007	0.0038	0.0986 ± 0.0151	$f_0^T(q^2_{\rm max})$	∞	0.0026 ± 0.0021	∞	∞
$f_\perp^T(0)$	0.046 ± 0.006	0.0030	0.0690 ± 0.0077	$f_\perp^T(q^2_{\rm max})$	∞	0.246 ± 0.007	∞	∞
$f_g^T(0)$	0.032 ± 0.006	-0.0041	0.0130 ± 0.0376	$f_g^T(q^2_{\rm max})$	0.234 ± 0.008	0.234 ± 0.008	-0.1509	-0.1506 ± 0.0127
$f_0^{T5}(0)$	0.040 ± 0.005	0.0032	-0.1207 ± 0.0500	$f_0^{T5}(q^2_{\rm max})$	0.211 ± 0.005	0.211 ± 0.005	0.1861	0.1412 ± 0.0127
$f_\perp^{T5}(0)$	0.038 ± 0.004	0.0030	-0.1333 ± 0.0471	$f_\perp^{T5}(q^2_{\rm max})$	0.178 ± 0.004	0.178 ± 0.004	0.1897	0.1476 ± 0.0127
$f_g^{T5}(0)$	-0.19 ± 0.05	0.0072	1.167 ± 0.688	$f_g^{T5}(q^2_{\rm max})$	-0.86 ± 0.06	-0.86 ± 0.06	-0.3268	-0.5826 ± 0.0918

[a]These results, listed in the fourth column, are obtained by the first extrapolation scheme. Here, the $f^V_{t,g}$, $f^A_{t,0,\perp,g}$, f^T_g, and $f^{T5}_{0,\perp,g}$ are extrapolated by Eq. (5.4), while the $f^V_{0,\perp}$ and $f^T_{0,\perp}$ are extrapolated by Eq. (5.7).

[b]These results, shown in the fifth column, are from the second extrapolation scheme. Here, all form factors are extrapolated by Eq. (5.4).

In the low-recoil limit, where HQET is valid [83–86], the weak transition matrix element can be re-expressed by two Isgur-Wise functions as [30,32,86]

$$\langle \Lambda^*(p')|\bar{s}\Gamma b|\Lambda_b(p)\rangle = \bar{u}^\alpha_\Lambda(p')v_\alpha[\zeta_1(\omega) + \not{v}\zeta_2(\omega)]\Gamma u_{\Lambda_b}(p). \tag{5.8}$$

Here, Γ is an arbitrary Dirac structure, and $\omega = v\cdot v' = (m^2_{\Lambda_b} + m^2_{\Lambda^*} - q^2)/(2m_{\Lambda_b}m_{\Lambda^*})$, where $v = p/m_{\Lambda_b}$ and $v' = p'/m_{\Lambda^*}$ represent the four velocities of the bottom baryon and hyperon, respectively. The eight form factors are derived as two independent form factors $\zeta_1(\omega)$ and $\zeta_2(\omega)$. In the low-recoil limit this gives $q^2 \to q^2_{\rm max} \equiv (m_{\Lambda_b} - m_{\Lambda^*})^2$ (or $\omega \to 1$). With slightly different definitions of the form factors in Refs. [25,60,87], we have [31]

$$\begin{aligned}
f_t^V(q^2_{\rm max}) &\simeq f_0^A(q^2_{\rm max}) \simeq f_\perp^A(q^2_{\rm max}) \\
&\simeq f_0^{T5}(q^2_{\rm max}) \simeq f_\perp^{T5}(q^2_{\rm max}) \simeq [\zeta_1(1) + \zeta_2(1)]/m_{\Lambda_b}, \\
f_0^V(q^2_{\rm max}) &\simeq f_t^A(q^2_{\rm max}) \simeq f_\perp^V(q^2_{\rm max}) \\
&\simeq f_0^T(q^2_{\rm max}) \simeq f_\perp^T(q^2_{\rm max}) \simeq [\zeta_1(1) - \zeta_2(1)]/m_{\Lambda_b}, \\
f_g^V(q^2_{\rm max}) &\simeq f_g^A(q^2_{\rm max}) \simeq f_g^T(q^2_{\rm max}) \simeq f_g^{T5}(q^2_{\rm max}) \simeq 0,
\end{aligned} \tag{5.9}$$

while in the large-recoil limit where SCET is valid, we have [60,87,88]

$$\langle \Lambda^*(p')|\bar{s}\Gamma b|\Lambda_b(p)\rangle = \bar{u}^\alpha_\Lambda(p')v_\alpha[\zeta(\omega)]\Gamma u_{\Lambda_b}(p), \tag{5.10}$$

where $\zeta(\omega)$ is the only remaining form factor. This gives, in the large-recoil limit, $q^2 \to 0$ (or $\omega \to (m^2_{\Lambda_b} + m^2_{\Lambda^*})/(2m_{\Lambda_b}m_{\Lambda^*})$),

$$\begin{aligned}
f_t^V(0) &\simeq f_0^V(0) \simeq f_\perp^V(0) \simeq f_t^A(0) \simeq f_0^A(0) \simeq f_\perp^A(0) \\
&\simeq f_0^T(0) \simeq f_\perp^T(0) \simeq f_0^{T5}(0) \simeq f_\perp^{T5}(0) \\
&\simeq \zeta\left(\frac{m^2_{\Lambda_b} + m^2_{\Lambda^*}}{2m_{\Lambda_b}m_{\Lambda^*}}\right)/m_{\Lambda_b},
\end{aligned} \tag{5.11}$$

and four f_g form factors will disappear. From Fig. 2, we can see that apart from the $f_g^{T(T5)}(q^2)$, which deviates from the predictions, the remaining calculated form factors are consistent with the requirements of HQET and SCET.

In addition, Bordone has completed the heavy quark expansion (HQE) calculation of the $\Lambda_b \to \Lambda^*$ form factors beyond the leading order [30]. At the zero-recoil limit, the HQE predicts the ratios of the form factors, which are independent of the Isgur-Wise functions, as [30]

$$\begin{aligned}
\frac{F_{1/2,0}}{F_{1/2,\perp}} &= \frac{F_{1/2,0}}{F_{3/2,\perp}} = -2\frac{m_{\Lambda_b} - m_{\Lambda^*}}{m_{\Lambda_b} + m_{\Lambda^*}} = -1.15, \\
\frac{F_{1/2,\perp}}{F_{3/2,\perp}} &= 1, \qquad \frac{T_{1/2,0}}{T_{1/2,\perp}} = -2\frac{m_{\Lambda_b} + m_{\Lambda^*}}{m_{\Lambda_b} - m_{\Lambda^*}} = -3.48, \\
\frac{T_{1/2,0}}{T_{3/2,\perp}} &= \frac{2m_{\Lambda^*}}{m_{\Lambda_b} - m_{\Lambda^*}} = 0.74, \\
\frac{T_{1/2,\perp}}{T_{3/2,\perp}} &= -\frac{m_{\Lambda^*}}{m_{\Lambda_b} + m_{\Lambda^*}} = -0.21.
\end{aligned} \tag{5.12}$$

Note that the form factor base used in Ref. [30] is different from ours. By using the conversions collected in Appendix B of Ref. [30] and Eq. (5.2), we can get our results of these ratios as

$$\begin{aligned}
\frac{F^{\text{this work}}_{1/2,0}}{F^{\text{this work}}_{1/2,\perp}} &= \frac{f_0^V}{f_\perp^V} = 0.521 \pm 0.026, \\
\frac{F^{\text{this work}}_{1/2,\perp}}{F^{\text{this work}}_{3/2,\perp}} &= -\frac{s_-}{m_{\Lambda^*}}\frac{f_\perp^V}{f_g^V} = -33.8 \pm 0.9, \\
\frac{F^{\text{this work}}_{1/2,0}}{F^{\text{this work}}_{3/2,\perp}} &= -\frac{s_-}{m_{\Lambda^*}}\frac{f_0^V}{f_g^V} = -17.6 \pm 0.7, \\
\frac{T^{\text{this work}}_{1/2,0}}{T^{\text{this work}}_{1/2,\perp}} &= \frac{f_0^T}{f_\perp^T} = -0.63 \pm 0.04, \\
\frac{T^{\text{this work}}_{1/2,0}}{T^{\text{this work}}_{3/2,\perp}} &= s_-\frac{f_0^T}{f_g^T} = -2.56 \pm 0.09, \\
\frac{T^{\text{this work}}_{1/2,\perp}}{T^{\text{this work}}_{3/2,\perp}} &= s_-\frac{f_\perp^T}{f_g^T} = 4.09 \pm 0.28.
\end{aligned} \tag{5.13}$$

Our results are very different from those of the HQE.

In addition, we also compare our results of the form factors with the NRQM [22] and the LQCD [29] at $q^2 = 0$ and $q^2 = q^2_{\rm max}$ endpoints in Table VI. Until now, less work has been done on the $\Lambda_b \to \Lambda(1520)$ transition, so more theoretical work is needed to validate these form factors.

B. The branching ratio and angular observables

With the above preparations, we will present our numerical results. The baryon and lepton masses used in our calculation are taken from the PDG [58], as well as $\tau_{\Lambda_b} = 1.470$ ps. We also use $\mathcal{B}_{\Lambda^*} \equiv \mathcal{B}(\Lambda^* \to N\bar{K}) = 45\%$ [58]. To compare with the experimental data, we examine a number of angular observables, including the CP-averaged normalized angular coefficients, the differential branching ratios, the lepton's forward-backward asymmetry (A^ℓ_{FB}), and the transverse (F_T) and longitudinal (F_L) polarization fractions of the dilepton system.

First, we examine the CP-averaged normalized angular distributions

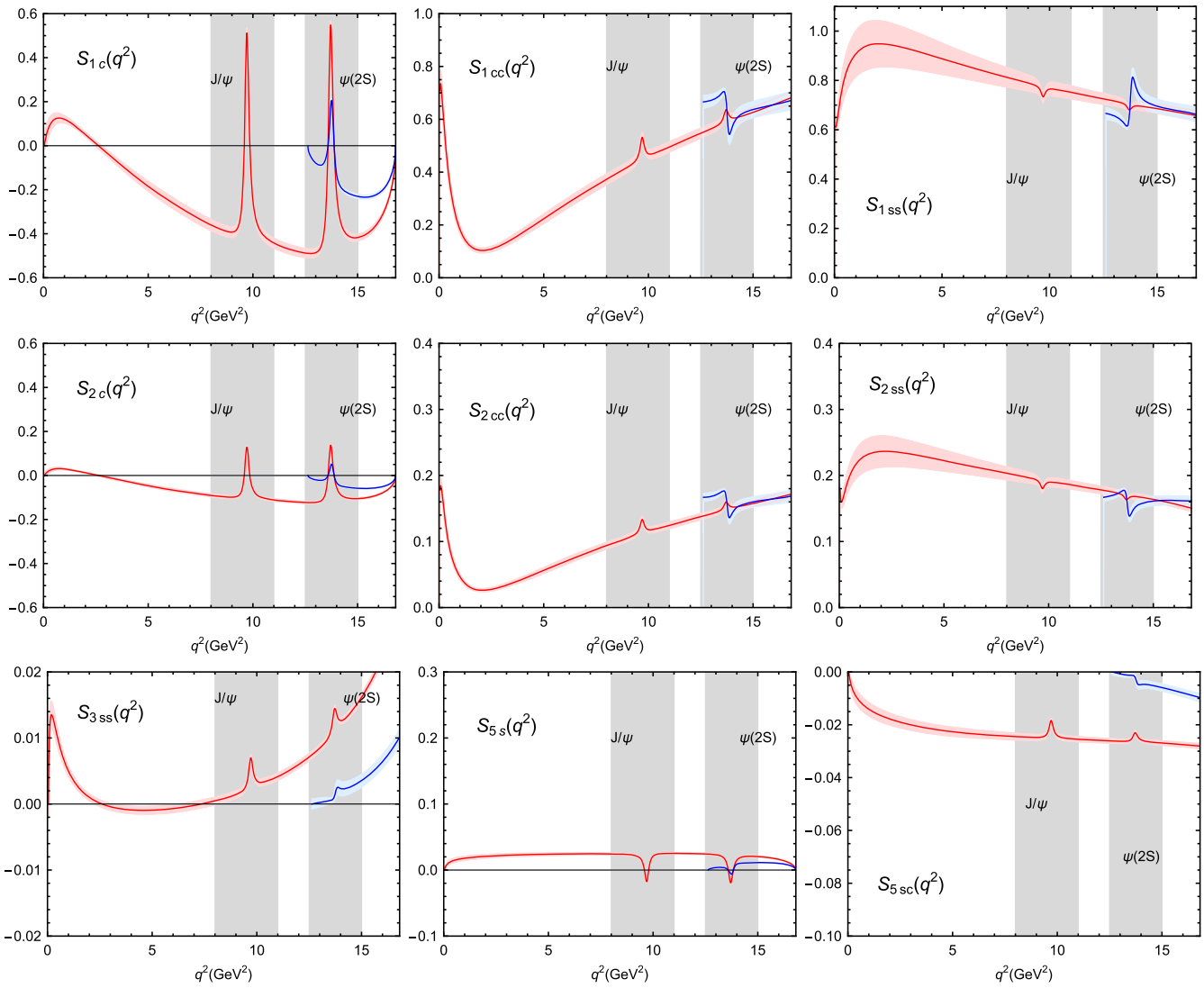

FIG. 3. The q^2 dependence of the normalized angular coefficients S_{1c}, S_{1cc}, S_{1ss}, S_{2c}, S_{2cc}, S_{2ss}, S_{3ss}, S_{5s}, and S_{5sc}. Here, the red curve and the blue curve are our results of the μ and τ channels, respectively, and the concomitant shadows are corresponding errors.

$$S_i = \frac{L_i + \bar{L}_i}{d(\Gamma + \bar{\Gamma})/dq^2}, \tag{5.14}$$

where the angular distributions L_i and the differential decay width $d\Gamma/dq^2$ are defined in Eqs. (2.34) and (2.35), respectively. For the CP-conjugated mode, the corresponding expression for the angular decay distribution should be written as

$$\frac{d^4\bar{\Gamma}}{dq^2 d\cos\theta_{\Lambda^*} d\cos\theta_\ell d\phi} = \frac{3}{8\pi}\sum_i \bar{L}_i(q^2) f_i(q^2, \theta_\ell, \theta_{\Lambda^*}, \phi), \tag{5.15}$$

where $\bar{L}_i(q^2)$ can be obtained by doing the full conjugation for all weak phases in $L_i(q^2)$. We should also do the substitutions as

$$\begin{aligned} &L_{1c,2c} \to -\bar{L}_{1c,2c}, \qquad L_{1cc,1ss,2cc,2ss} \to \bar{L}_{1cc,1ss,2cc,2ss}, \\ &L_{3ss} \to \bar{L}_{3ss}, \qquad L_{4ss} \to -\bar{L}_{4ss}, \\ &L_{5s} \to -\bar{L}_{5s}, \qquad L_{5sc} \to \bar{L}_{5sc}, \\ &L_{6s} \to \bar{L}_{6s}, \qquad L_{6sc} \to -\bar{L}_{6sc}, \end{aligned} \tag{5.16}$$

where the minus sign is a result from the operations of $\theta_\ell \to \theta_\ell - \pi$ and $\phi \to -\phi$. The differential decay width of the conjugated mode is

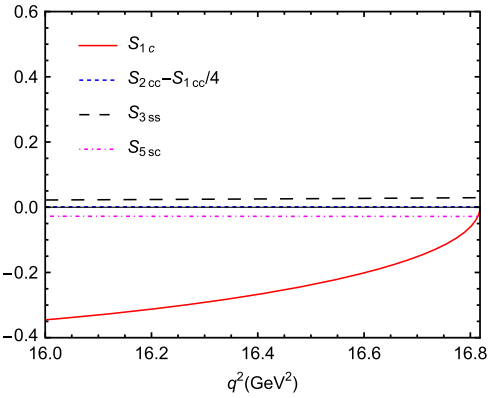

FIG. 4. The behaviors of the normalized angular coefficients S_{1c}, $S_{2cc}-S_{1cc}/4$, S_{3ss}, and S_{5sc} in the low-recoil region with $m_\ell = 0$.

$$\frac{d\bar{\Gamma}}{dq^2} = \frac{1}{3}(\bar{L}_{1cc} + 2\bar{L}_{1ss} + 2\bar{L}_{2cc} + 4\bar{L}_{2ss} + 2\bar{L}_{3ss}). \quad (5.17)$$

In Fig. 3, we present our results for the q^2 dependent normalized angular coefficients. Since the e channel shows similar behavior to the μ channel, we only present the results of the μ and the τ channels here. These angular distributions are important physical observables, and can be checked by future experiments.

At the low-recoil endpoint for $q^2 \to (m_{\Lambda_b} - m_{\Lambda^*})^2$, Descotes-Genon and Novoa-Brunet predicted [31]

$$S_{1c} \to 0, \qquad S_{2cc} - S_{1cc}/4 \to 3/8,$$
$$S_{3ss} \to -1/4, \qquad S_{5sc} \to -1/2$$

by neglecting the contribution from the photon pole. In Fig. 4, we present the behavior of the normalized angular coefficients S_{1c}, $S_{2cc}-S_{1cc}/4$, S_{3ss}, and S_{5sc} in the low-recoil region by assuming $m_\ell = 0$. It is obvious that our result for S_{1c} is strictly consistent with the above prediction, while the $S_{2cc} - S_{1cc}/4$, S_{3ss}, and S_{5sc} show apparent deviations.

We further evaluate the differential branching ratios using Eq. (2.35). The q^2 dependence of the differential branching ratios is shown in Fig. 5, where the orange solid curve, the blue dashed curve, and the purple dot-dashed curve are our results for the e, μ, and τ channels, respectively. The gray zones in the regions of the dilepton mass squared $8.0 < q^2 < 11.0\ \mathrm{GeV}^2$ and $12.5 < q^2 < 15.0\ \mathrm{GeV}^2$ show the contributions from the charmonium resonances J/ψ and $\psi(2S)$, respectively.

Recently, the LHCb collaboration measured the "non-resonant" contributions, which are different from the "resonant" contribution from $\Lambda_b^0 \to pK^- J\psi(\to \ell^+\ell^-)$, to $\mathcal{B}(\Lambda_b^0 \to pK^- e^+ e^-)$ and $\mathcal{B}(\Lambda_b^0 \to pK^-\mu^+\mu^-)$ decays as

$$\mathcal{B}(\Lambda_b^0 \to pK^- e^+ e^-) = (3.1 \pm 0.4 \pm 0.2 \pm 0.3^{+0.4}_{-0.3}) \times 10^{-7},$$
$$\mathcal{B}(\Lambda_b^0 \to pK^-\mu^+\mu^-) = (2.65 \pm 0.14 \pm 0.12 \pm 0.29^{+0.38}_{-0.23}) \times 10^{-7},$$

in the region of $0.1 \le q^2 \le 6\ \mathrm{GeV}^2/c^4$ and $m(pK^-) < 2600\ \mathrm{MeV}/c^2$ [89]. Assuming $\mathcal{B}(\Lambda(1520) \to pK^-) = \mathcal{B}(\Lambda(1520) \to n\bar{K}^0)$, we calculate

$$\mathcal{B}(\Lambda_b^0 \to \Lambda^*(\to pK^-)e^+e^-)_{0.1\le q^2\le 6\ \mathrm{GeV}^2} = (1.618 \pm 0.108) \times 10^{-7},$$
$$\mathcal{B}(\Lambda_b^0 \to \Lambda^*(\to pK^-)\mu^+\mu^-)_{0.1\le q^2\le 6\ \mathrm{GeV}^2} = (1.610 \pm 0.106) \times 10^{-7}.$$

This indicates that the contribution from $\Lambda(1520)$ is significant. We find from the PDG [58] that $\Lambda(1600)$, $\Lambda(1670)$, and other hyperons can also decay to the $N\bar{K}$ final state. Their contributions need to be carefully studied. Further studies with more excited Λ hyperons will make a difference to the $\Lambda_b^0 \to pK^-\ell^+\ell^-$ decays.

In addition, the q^2 dependence of the lepton-side forward-backward asymmetry (A_{FB}^ℓ), and the transverse (F_T) and

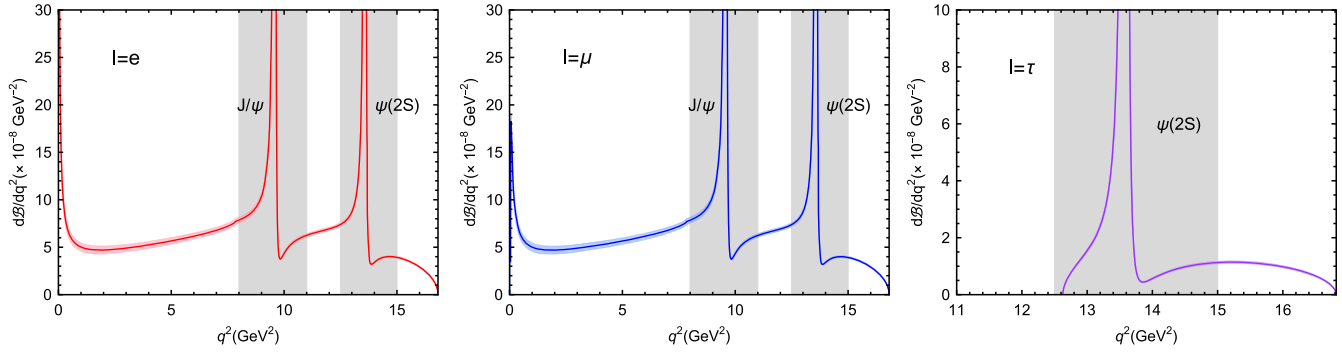

FIG. 5. The q^2 dependence of the differential branching ratios for $\Lambda_b \to \Lambda^*(\to N\bar{K})\ell^+\ell^-$ [$\ell = e$(left panel), μ(center panel), τ(right panel)], where the red, the blue, and the purple curves are our results from the e, μ, and τ channels, respectively, and the concomitant shadows are the corresponding errors.

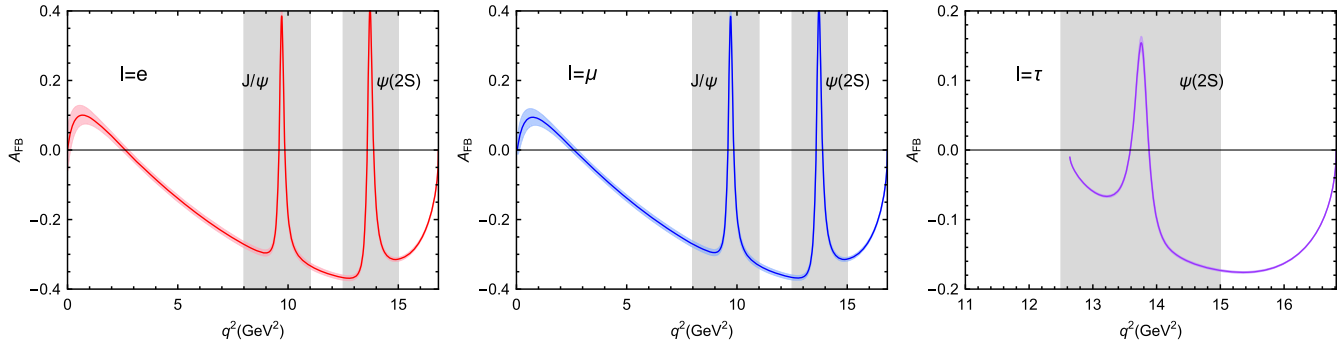

FIG. 6. The q^2 dependence of the lepton-side forward-backward asymmetry parameter (A_{FB}^{ℓ}) for $\Lambda_b \to \Lambda^*(\to N\bar{K})\ell^+\ell^-$ [$\ell = e$(left panel), μ(center panel), τ(right panel)], where the red, blue, and purple curves are our results from the e, μ, and τ channels, respectively, and the shadows are the corresponding errors.

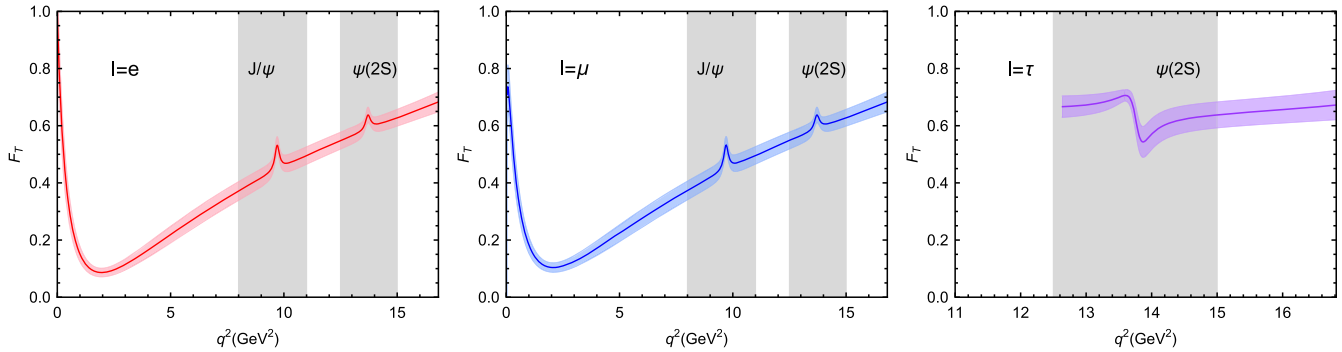

FIG. 7. The q^2 dependence of the transverse polarization fractions (F_T) for $\Lambda_b \to \Lambda^*(\to N\bar{K})\ell^+\ell^-$ [$\ell = e$(left panel), μ(center panel), τ(right panel)], where the red, blue, and purple curves are our results of the e, μ, and τ channels, respectively, and the shadows are the corresponding errors.

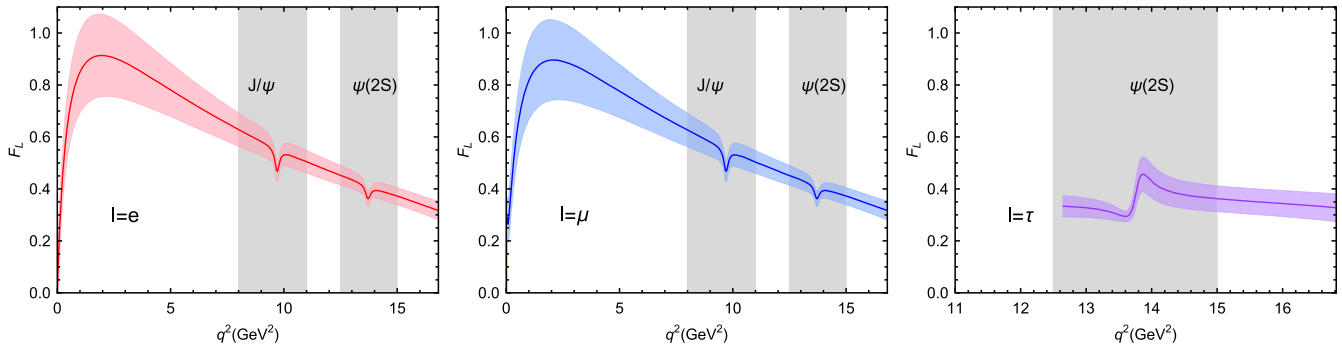

FIG. 8. The q^2 dependence of the longitudinal polarization fractions (F_L) for $\Lambda_b \to \Lambda^*(\to N\bar{K})\ell^+\ell^-$ ($\ell = e$(left panel), μ(center panel), τ(right panel)), where the red, blue, and purple curves are our results of the e, μ, and τ channels, respectively, and the shadows are the corresponding errors.

longitudinal (F_L) polarization fractions of the dilepton system are presented in Figs. 6, 7, and 8, respectively, where we also show the contributions from the charmonium resonances J/ψ and $\psi(2S)$ with gray zones. The averaged values of these angular observables for the e and μ channels defined in Eq. (2.39) in the region of $0.1 < q^2 < 6.0$ GeV^2 are presented in Table VII. The angular distributions provide a rich set of physical observables to study the weak interaction and the structure of $\Lambda(1520)$, and are also important to study the NP effects beyond the SM [24,31,32,36,51], so we call for the ongoing LHCb experiment to measure them.

TABLE VII. The predictions for the averaged lepton-side forward-backward asymmetry $\langle A_{FB}^{\ell}\rangle$, the averaged transverse polarization fraction $\langle F_T\rangle$, and the averaged longitudinal polarization fraction $\langle F_L\rangle$ in the region of $0.1 < q^2 < 6.0\ \mathrm{GeV}^2$.

Channels	$\langle A_{FB}^{\ell}\rangle$	$\langle F_T\rangle$	$\langle F_L\rangle$
$\ell = e$	-0.030 ± 0.012	0.208 ± 0.055	0.792 ± 0.231
$\ell = \mu$	-0.032 ± 0.010	0.221 ± 0.057	0.779 ± 0.225

VI. SUMMARY

With the accumulation of experimental data in the LHCb Collaboration, the experimental exploration of rare decays $b \to s\ell^+\ell^-$ ($\ell = e, \mu, \tau$) in the baryon sector, especially the P-wave final state $\Lambda_b \to \Lambda(1520)\ell^+\ell^-$, will attract more attention. Given this opportunity, in this work we focus on the quasi-four-body decay $\Lambda_b \to \Lambda(1520)(\to N\bar{K})\ell^+\ell^-$, where the angular coefficients, the differential branching ratio, and several angular observables, including the lepton-side forward-backward asymmetry (A_{FB}^{ℓ}), and the transverse and longitudinal polarization fractions ($F_{T(L)}$) are investigated.

To describe the weak process, we have worked in the helicity formula, where the relevant weak transition form factors are obtained through the three-body light-front quark model. Our main advantage is the improved treatment of the spatial wave functions of the involved baryons, where a semirelativistic potential model is applied to solve the numerical spatial wave functions of the baryons assisted by the GEM. Thus, we emphasize that our study of the rare decay $\Lambda_b \to \Lambda(1520)(\to N\bar{K})\ell^+\ell^-$ is supported by the baryon spectroscopy. Our results of the form factors are comparable with the predictions of HQET and SCET, and also with the calculations by the LQCD approach. These form factors will be useful for the study of the corresponding weak decays.

Overall, we have systematically investigated the $\Lambda_b \to \Lambda(1520)(\to N\bar{K})\ell^+\ell^-$ ($\ell = e, \mu, \tau$) processes in the framework of the three-body light-front quark model based on the Gaussian expansion method. We believe that the present work can serve as an essential step toward strong dynamics on the beauty baryon decays. We expect that under the considerable progress on the experimental side, the above predictions could be tested by future LHCb experiments.

ACKNOWLEDGMENTS

We would like to thank Prof. Yu-Ming Wang, Prof. Wei Wang, and Dr. Si-Qiang Luo for helpful discussions. This work is supported by the China National Funds for Distinguished Young Scientists under Grant No. 11825503, the National Key Research and Development Program of China under Contract No. 2020YFA0406400, the 111 Project under Grant No. B20063, the National Natural Science Foundation of China under Grant No. 12047501, the Project for top-notch innovative talents of Gansu province, and by the Fundamental Research Funds for the Central Universities under Grant No. lzujbky-2022-it17. J. G. is also supported by the National Natural Science Foundation of China under Grant No. 12147118.

APPENDIX A: THE DIFFERENTIAL DECAY WIDTH

The differential decay width for the quasi-four-body decay $\Lambda_b \to \Lambda^*(\to N\bar{K})\ell^+\ell^-$ is

$$d\Gamma = \frac{|\mathcal{M}|^2}{2m_{\Lambda_b}} d\Phi_4(p; k_1, k_2, q_1, q_2), \tag{A1}$$

where $d\Phi_4$ is the four-body phase space given by

$$\begin{aligned} &d\Phi_4(p; k_1, k_2, q_1, q_2) \\ &= (2\pi)^4\delta^4(p - k_1 - k_2 - q_1 - q_2) \\ &\quad\times \prod_{i=1}^{2}\frac{d^3\vec{k}_i}{(2\pi)^3 2E_{k_i}} \prod_{j=1}^{2}\frac{d^3\vec{q}_j}{(2\pi)^3 2E_{q_j}} \\ &= \frac{dk^2}{2\pi}\frac{dq^2}{2\pi} d\Phi_2(k; k_1, k_2) d\Phi_2(q; q_1, q_2) d\Phi_2(p; k, q), \end{aligned} \tag{A2}$$

where the two-body phase spaces are written as

$$\begin{aligned} \int d\Phi_2(k; k_1, k_2) &= \frac{1}{32\pi^2}\frac{\sqrt{\lambda(k^2, k_1^2, k_2^2)}}{k^2}\int_{-1}^{1} d\cos\theta_{\Lambda^*}\int_0^{2\pi} d\phi, \\ \int d\Phi_2(q; q_1, q_2) &= \frac{1}{32\pi^2}\frac{\sqrt{\lambda(q^2, q_1^2, q_2^2)}}{q^2}\int_{-1}^{1} d\cos\theta_{\ell}\times(2\pi), \\ \int d\Phi_2(p; k, q) &= \frac{1}{32\pi^2}\frac{\sqrt{\lambda(p^2, k^2, q^2)}}{p^2}\times 2\times(2\pi). \end{aligned} \tag{A3}$$

As shown in Fig. 9, three angles are defined: (i) the angle θ_{Λ^*} is defined as the angle that the nucleon makes with the $+z$ axis in the $(N\bar{K})$ center of mass system, (ii) the angle θ_ℓ is defined as the angle made by the ℓ^- with the $+z$ axis in the $(\ell^+\ell^-)$ center of mass system, and (iii) the angle ϕ between the two decay planes, respectively.

The decay width of the concerned decay $\Lambda_b \to \Lambda^*(\to N\bar{K})\ell^+\ell^-$ is expressed as

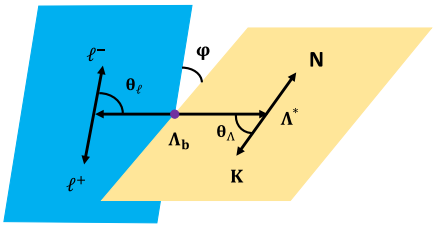

FIG. 9. Kinematics of the four-body $\Lambda_b \to \Lambda^*(\to N\bar{K})\ell^+\ell^-$ decay, where the angles are defined in the corresponding rest frames.

$$\int d\Phi_4 \frac{|\mathcal{M}|^2}{2m_{\Lambda_b}} = \frac{2}{(32\pi^2)^3}\int dk^2 \frac{\sqrt{\lambda(k^2,k_1^2,k_2^2)}}{k^2}\frac{\sqrt{\lambda(q^2,q_1^2,q_2^2)}}{q^2}\times\frac{\sqrt{\lambda(p^2,k^2,q^2)}}{p^2}(dq^2 d\cos\theta_{\Lambda^*} d\cos\theta_\ell d\phi)\frac{|\mathcal{M}|^2}{2m_{\Lambda_b}}. \quad \text{(A4)}$$

We also take into account the width of Λ^* to modify its propagator, but treat it as narrow ($\Gamma_{\Lambda^*} \ll m_{\Lambda^*}$) state.[2] This gives [24]

$$\begin{aligned}
\int d\Phi_4 \frac{|\mathcal{M}|^2}{2m_{\Lambda_b}} &= \int d\Phi_4 \frac{|\mathcal{M}|^2}{2m_{\Lambda_b}} \frac{1}{(k^2-m_{\Lambda^*}^2)^2}(k^2-m_{\Lambda^*}^2)^2 \\
&\overset{\Gamma_{\Lambda^*}\ll m_{\Lambda^*}}{\longrightarrow} \int d\Phi_4 \frac{|\mathcal{M}|^2}{2m_{\Lambda_b}} \frac{(k^2-m_{\Lambda^*}^2)^2}{(k^2-m_{\Lambda^*}^2)^2+(m_{\Lambda^*}\Gamma_{\Lambda^*})^2} \\
&= \int d\Phi_4 \frac{|\mathcal{M}|^2}{2m_{\Lambda_b}} \frac{(k^2-m_{\Lambda^*}^2)^2}{m_{\Lambda^*}^3\Gamma_{\Lambda^*}} \frac{\Gamma_{\Lambda^*}/m_{\Lambda^*}}{\frac{\Gamma_{\Lambda^*}^2}{m_{\Lambda^*}^2}+\left(\frac{k^2}{m_{\Lambda^*}^2}-1\right)^2} \\
&\overset{\Gamma_{\Lambda^*}\ll m_{\Lambda^*}}{\longrightarrow} \int d\Phi_4 \frac{|\mathcal{M}|^2}{2m_{\Lambda_b}} (k^2-m_{\Lambda^*}^2)^2 \frac{\pi}{m_{\Lambda^*}^3\Gamma_{\Lambda^*}}\delta\left(\frac{k^2}{m_{\Lambda^*}^2}-1\right) \\
&= \int d\Phi_4 \frac{|\mathcal{M}|^2}{2m_{\Lambda_b}} (k^2-m_{\Lambda^*}^2)^2 \frac{\pi}{m_{\Lambda^*}\Gamma_{\Lambda^*}}\delta(k^2-m_{\Lambda^*}^2), \quad \text{(A5)}
\end{aligned}$$

with the properties of the Dirac delta function,

$$\begin{aligned}
\lim_{\epsilon\to 0}\frac{\epsilon}{\epsilon^2+x^2} &= \pi\delta(x), \\
\delta\left(\frac{k^2}{m_{\Lambda^*}^2}-1\right) &= m_{\Lambda^*}^2\delta(k^2-m_{\Lambda^*}^2), \quad \text{(A6)}
\end{aligned}$$

applied.

Following the above discussion, we can finally obtain

$$\begin{aligned}
\int d\Phi_4 \frac{|\mathcal{M}|^2}{2m_{\Lambda_b}} = \frac{1}{2^{15}\pi^5 m_{\Lambda_b} m_{\Lambda^*}\Gamma_{\Lambda^*}} &\int dq^2 d\cos\theta_\Lambda d\cos\theta_\ell d\phi \frac{\sqrt{\lambda(k^2,k_1^2,k_2^2)}}{k^2}\frac{\sqrt{\lambda(q^2,q_1^2,q_2^2)}}{q^2}\frac{\sqrt{\lambda(p^2,k^2,q^2)}}{p^2} \\
&\times (k^2-m_{\Lambda^*})^2 |\mathcal{M}|^2|_{k^2=m_{\Lambda^*}^2}, \quad \text{(A7)}
\end{aligned}$$

where $\lambda(x,y,z) = x^2+y^2+z^2-2xy-2xz-2yz$ is the kinematic triangle Källén function.

APPENDIX B: THE KINEMATIC CONVENTIONS

In this paper, we assign the particle momenta and spin variables for the hadrons in the $\Lambda_b \to \Lambda^*(\to N\bar{K})\ell^+\ell^-$ process according to

$$\begin{aligned}
\Lambda_b(p,s_{\Lambda_b}) &\to \Lambda^*(k,s_{\Lambda^*})\ell^-(q_1,s_\ell)\nu_\ell(q_2,s_\nu), \\
\Lambda^*(k,s_{\Lambda^*}) &\to N(k_1,s_N)\bar{K}(k_2), \quad \text{(B1)}
\end{aligned}$$

as shown in Fig. 9. Here we have some relations like $q^\mu = q_1^\mu + q_2^\mu$, $k^\mu = k_1^\mu + k_2^\mu$, and $p^\mu = k^\mu + q^\mu$.

[2]Checking the PDG [58], we notice that $m_{\Lambda(1520)} = 1519$ MeV and $\Gamma_{\Lambda(1520)} = 16$ MeV, indicating that it is reasonable to take the narrow-width approximation.

In the following, we will introduce some kinematic conventions that are useful for the calculation of the involved helicity amplitudes.

1. Some conventions in Λ_b rest frame

In the Λ_b rest frame, we have the four-momentum of Λ_b, Λ^* and the vector boson as

$$\begin{aligned}
p^\mu &= (m_{\Lambda_b}, 0, 0, 0), \\
k^\mu &= (E_{\Lambda^*}, 0, 0, |\vec{p}_{\Lambda^*}|), \\
q^\mu &= (q_0, 0, 0, -|\vec{q}|), \quad \text{(B2)}
\end{aligned}$$

where

$$E_{\Lambda^*}=\frac{m_{\Lambda_b}^2+m_{\Lambda^*}^2-q^2}{2m_{\Lambda_b}},\qquad |\vec{p}_{\Lambda^*}|=|\vec{q}|=\frac{\sqrt{s_+s_-}}{2m_{\Lambda_b}},$$
$$q_0=\frac{m_{\Lambda_b}^2-m_{\Lambda^*}^2+q^2}{2m_{\Lambda_b}},\qquad s_\pm=(m_{\Lambda_b}\pm m_{\Lambda^*})^2-q^2. \tag{B3}$$

We have the following solutions for the Dirac spinor of Λ_b for different s_{Λ_b} as

$$u_{\Lambda_b}(-1/2)=\begin{pmatrix}\sqrt{2m_{\Lambda_b}}\\0\\0\\0\end{pmatrix},\quad u_{\Lambda_b}(+1/2)=\begin{pmatrix}0\\\sqrt{2m_{\Lambda_b}}\\0\\0\end{pmatrix}, \tag{B4}$$

and the solutions for the Rarita-Schwinger spinor $u_{\Lambda^*,\alpha}(s_{\Lambda^*})$ for different s_{Λ^*} as [31]

$$u_{\Lambda^*}\left(-\frac{3}{2}\right)=\frac{1}{2\sqrt{m_{\Lambda_b}}}\begin{pmatrix}0&0&0&0\\0&\sqrt{s_+}&0&-\sqrt{s_-}\\0&-i\sqrt{s_+}&0&i\sqrt{s_-}\\0&0&0&0\end{pmatrix},$$
$$u_{\Lambda^*}\left(-\frac{1}{2}\right)=\frac{\sqrt{s_-s_+}}{4\sqrt{3}m_{\Lambda^*}m_{\Lambda_b}^{3/2}}\begin{pmatrix}0&2\sqrt{s_+}&0&-2\sqrt{s_-}\\\frac{2m_{\Lambda^*}m_{\Lambda_b}}{\sqrt{s_-}}&0&\frac{2m_{\Lambda^*}m_{\Lambda_b}}{\sqrt{s_+}}&0\\\frac{-2im_{\Lambda^*}m_{\Lambda_b}}{\sqrt{s_-}}&0&\frac{-2im_{\Lambda^*}m_{\Lambda_b}}{\sqrt{s_+}}&0\\0&\frac{s_-+s_+}{\sqrt{s_-}}&0&-\frac{s_-+s_+}{\sqrt{s_+}}\end{pmatrix},$$
$$u_{\Lambda^*}\left(+\frac{1}{2}\right)=\frac{\sqrt{s_-s_+}}{4\sqrt{3}m_{\Lambda^*}m_{\Lambda_b}^{3/2}}\begin{pmatrix}2\sqrt{s_+}&0&2\sqrt{s_-}&0\\0&\frac{-2m_{\Lambda^*}m_{\Lambda_b}}{\sqrt{s_-}}&0&\frac{2m_{\Lambda^*}m_{\Lambda_b}}{\sqrt{s_+}}\\0&\frac{-2im_{\Lambda^*}m_{\Lambda_b}}{\sqrt{s_-}}&0&\frac{2im_{\Lambda^*}m_{\Lambda_b}}{\sqrt{s_+}}\\\frac{s_-+s_+}{\sqrt{s_-}}&0&\frac{s_-+s_+}{\sqrt{s_+}}&0\end{pmatrix},$$
$$u_{\Lambda^*}\left(+\frac{3}{2}\right)=\frac{1}{2\sqrt{m_{\Lambda_b}}}\begin{pmatrix}0&0&0&0\\-\sqrt{s_+}&0&-\sqrt{s_-}&0\\-i\sqrt{s_+}&0&-i\sqrt{s_-}&0\\0&0&0&0\end{pmatrix}, \tag{B5}$$

where the column and row notations correspond to the spinor indices α and the vector indices, respectively. In addition, the polarization vectors for the virtual vector boson alone on the $-z$ axis in the Λ_b rest frame are expressed as

$$\epsilon^\mu(t)=\frac{1}{\sqrt{q^2}}(q_0,0,0,-|\vec{q}|),$$
$$\epsilon^\mu(0)=\frac{1}{\sqrt{q^2}}(-|\vec{q}|,0,0,q_0),$$
$$\epsilon^\mu(\pm)=\frac{1}{\sqrt{2}}(0,\mp1,-i,0), \tag{B6}$$

where we use t and 0 to distinguish the two $\lambda_W=0$ states (0 for $J=1$ and t for $J=0$), and $\pm$ to represent $\lambda_W=\pm$ for $J=1$, respectively.

2. Some conventions in the dilepton rest frame

In the dilepton rest frame, we have the four-momentum of the vector bosons and leptons as

$$q^\mu=\left(\sqrt{q^2},0,0,0\right),$$
$$q^\mu_{\ell^-}=(E_\ell,|\vec{q}_\ell|\sin\theta_\ell,0,|\vec{q}_\ell|\cos\theta_\ell),$$
$$q^\mu_{\ell^+}=(E_\ell,-|\vec{q}_\ell|\sin\theta_\ell,0,-|\vec{q}_\ell|\cos\theta_\ell), \tag{B7}$$

where $|\vec{q}_\ell| = \sqrt{q^2}\beta_\ell/2$ and $E_\ell = \sqrt{q^2}/2$. The Dirac spinors for ℓ^- and ℓ^+ in Dirac representation are

$$u_{\ell^-}(\vec{q}_\ell, s_{\ell^-}) = \begin{pmatrix} \sqrt{E_\ell + m_\ell}\chi(\vec{q}_\ell, s_{\ell^-}) \\ 2s_{\ell^-}\sqrt{E_\ell - m_\ell}\chi(\vec{q}_\ell, s_{\ell^-}) \end{pmatrix},$$
$$v_{\ell^+}(-\vec{q}_\ell, s_{\ell^+}) = \begin{pmatrix} \sqrt{E_\ell - m_\ell}\xi(-\vec{q}_\ell, s_{\ell^+}) \\ -2s_{\ell^+}\sqrt{E_\ell + m_\ell}\xi(-\vec{q}_\ell, s_{\ell^+}) \end{pmatrix}, \quad \text{(B8)}$$

respectively, where

$$\chi\left(\vec{q}_\ell, \frac{1}{2}\right) = \xi\left(-\vec{q}_\ell, \frac{1}{2}\right) = \begin{pmatrix} \cos\frac{\theta_\ell}{2} \\ \sin\frac{\theta_\ell}{2} \end{pmatrix},$$
$$\chi\left(\vec{q}_\ell, -\frac{1}{2}\right) = -\xi\left(-\vec{q}_\ell, -\frac{1}{2}\right) = \begin{pmatrix} -\sin\frac{\theta_\ell}{2} \\ \cos\frac{\theta_\ell}{2} \end{pmatrix}. \quad \text{(B9)}$$

In addition, the polarization vectors of the virtual vector boson in the dilepton rest frame are written as

$$\bar{\epsilon}^\mu(t) = (1,0,0,0),$$
$$\bar{\epsilon}^\mu(0) = (0,0,0,1),$$
$$\bar{\epsilon}^\mu(\pm) = \frac{1}{\sqrt{2}}(0, \mp 1, -i, 0), \quad \text{(B10)}$$

which satisfy the following orthogonality and completeness relations [24,31,32]

$$\bar{\epsilon}^{*\mu}(m)\bar{\epsilon}_\mu(n) = \tilde{g}_{mn}, \quad \text{(B11)}$$

$$\sum_{m,n} \bar{\epsilon}^{*\mu}(m)\bar{\epsilon}^\nu(n)\tilde{g}_{mn} = g^{\mu\nu}, \quad \text{(B12)}$$

where $m, n \in \{t, \pm, 0\}$, $\tilde{g}_{mn} = \mathrm{diag}(+1,-1,-1,-1)$, and $g^{\mu\nu} = \mathrm{diag}(+1,-1,-1,-1)$.

3. Some conventions in Λ^* rest frame

In the Λ^* rest frame, we have the following solutions for the Rarita-Schwinger spinor $u_{\Lambda^*,\alpha}(s_{\Lambda^*})$ with different s_{Λ^*} as [31,32]

$$u_{\Lambda^*}(-3/2) = \sqrt{m_{\Lambda^*}}\begin{pmatrix} 0 & 0 & 0 & 0 \\ 0 & 1 & 0 & 0 \\ 0 & -i & 0 & 0 \\ 0 & 0 & 0 & 0 \end{pmatrix},$$
$$u_{\Lambda^*}(-1/2) = \sqrt{\frac{m_{\Lambda^*}}{3}}\begin{pmatrix} 0 & 0 & 0 & 0 \\ 1 & 0 & 0 & 0 \\ -i & 0 & 0 & 0 \\ 0 & 2 & 0 & 0 \end{pmatrix},$$
$$u_{\Lambda^*}(+1/2) = \sqrt{\frac{m_{\Lambda^*}}{3}}\begin{pmatrix} 0 & 0 & 0 & 0 \\ 0 & -1 & 0 & 0 \\ 0 & -i & 0 & 0 \\ 2 & 0 & 0 & 0 \end{pmatrix},$$
$$u_{\Lambda^*}(+3/2) = \sqrt{m_{\Lambda^*}}\begin{pmatrix} 0 & 0 & 0 & 0 \\ -1 & 0 & 0 & 0 \\ -i & 0 & 0 & 0 \\ 0 & 0 & 0 & 0 \end{pmatrix}, \quad \text{(B13)}$$

where the column and row notations correspond to the spinor indices α and the vector indices, respectively, and the solutions for the Dirac spinor of the nucleon for different s_N as

$$u_N(-1/2) = \frac{1}{2m_{\Lambda^*}}\begin{pmatrix} -\sqrt{r_+}\sin\frac{\theta_{\Lambda^*}}{2}e^{-i\phi} \\ \sqrt{r_+}\cos\frac{\theta_{\Lambda^*}}{2} \\ \sqrt{r_-}\sin\frac{\theta_{\Lambda^*}}{2}e^{-i\phi} \\ -\sqrt{r_-}\cos\frac{\theta_{\Lambda^*}}{2} \end{pmatrix},$$
$$u_N(+1/2) = \frac{1}{2m_{\Lambda^*}}\begin{pmatrix} \sqrt{r_+}\cos\frac{\theta_{\Lambda^*}}{2} \\ \sqrt{r_+}\sin\frac{\theta_{\Lambda^*}}{2}e^{i\phi} \\ \sqrt{r_-}\cos\frac{\theta_{\Lambda^*}}{2} \\ \sqrt{r_-}\sin\frac{\theta_{\Lambda^*}}{2}e^{i\phi} \end{pmatrix}. \quad \text{(B14)}$$

[1] M. Huschle *et al.* (Belle Collaboration), Measurement of the branching ratio of $\bar{B} \to D^{(*)}\tau^-\bar{\nu}_\tau$ relative to $\bar{B} \to D^{(*)}\ell^-\bar{\nu}_\ell$ decays with hadronic tagging at Belle, Phys. Rev. D **92**, 072014 (2015).

[2] R. Aaij *et al.* (LHCb Collaboration), Measurement of the Ratio of Branching Fractions $\mathcal{B}(\bar{B}^0 \to D^{*+}\tau^-\bar{\nu}_\tau)/\mathcal{B}(\bar{B}^0 \to D^{*+}\mu^-\bar{\nu}_\mu)$, Phys. Rev. Lett. **115**, 111803 (2015); **115**, 159901(E) (2015).

[3] S. Hirose *et al.* (Belle Collaboration), Measurement of the τ Lepton Polarization and $R(D^*)$ in the Decay $\bar{B} \to D^* \tau^- \bar{\nu}_\tau$, Phys. Rev. Lett. **118**, 211801 (2017).

[4] G. Caria *et al.* (Belle Collaboration), Measurement of $\mathcal{R}(D)$ and $\mathcal{R}(D^*)$ with a Semileptonic Tagging Method, Phys. Rev. Lett. **124**, 161803 (2020).

[5] T. M. Aliev, A. Ozpineci, and M. Savci, Exclusive $\Lambda_b \to \Lambda \ell^+ \ell^-$ decay beyond standard model, Nucl. Phys. **B649**, 168 (2003).

[6] D. Das, On the angular distribution of $\Lambda_b \to \Lambda(\to N\pi)\tau^+\tau^-$ decay, J. High Energy Phys. 07 (2018) 063.

[7] T. Aaltonen *et al.* (CDF Collaboration), Observation of the Baryonic Flavor-Changing Neutral Current Decay $\Lambda_b \to \Lambda \mu^+ \mu^-$, Phys. Rev. Lett. **107**, 201802 (2011).

[8] R. Aaij *et al.* (LHCb Collaboration), Differential branching fraction and angular analysis of $\Lambda_b^0 \to \Lambda \mu^+ \mu^-$ decays, J. High Energy Phys. 06 (2015) 115; 09 (2018) 145(E).

[9] R. Aaij *et al.* (LHCb Collaboration), Angular moments of the decay $\Lambda_b^0 \to \Lambda \mu^+ \mu^-$ at low hadronic recoil, J. High Energy Phys. 09 (2018) 146.

[10] G. Li, C. W. Liu, and C. Q. Geng, Bottomed baryon decays with invisible Majorana fermions, Phys. Rev. D **106**, 115007 (2022).

[11] W. Altmannshofer and F. Archilli, Rare decays of b and c hadrons, arXiv:2206.11331.

[12] W. Detmold and S. Meinel, $\Lambda_b \to \Lambda \ell^+ \ell^-$ form factors, differential branching fraction, and angular observables from lattice QCD with relativistic b quarks, Phys. Rev. D **93**, 074501 (2016).

[13] W. Detmold, C. J. D. Lin, S. Meinel, and M. Wingate, $\Lambda_b \to \Lambda \ell^+ \ell^-$ form factors and differential branching fraction from lattice QCD, Phys. Rev. D **87**, 074502 (2013).

[14] C. H. Chen and C. Q. Geng, Lepton asymmetries in heavy baryon decays of $\Lambda_b \to \Lambda \ell^+ \ell^-$, Phys. Lett. B **516**, 327 (2001).

[15] M. J. Aslam, Y. M. Wang, and C. D. Lü, Exclusive semileptonic decays of $\Lambda_b \to \Lambda \ell^+ \ell^-$ in supersymmetric theories, Phys. Rev. D **78**, 114032 (2008).

[16] Y. M. Wang and Y. L. Shen, Perturbative corrections to $\Lambda_b \to \Lambda$ form factors from QCD light-cone sum rules, J. High Energy Phys. 02 (2016) 179.

[17] T. M. Aliev, K. Azizi, and M. Savci, Analysis of the $\Lambda_b \to \Lambda \ell^+ \ell^-$ decay in QCD, Phys. Rev. D **81**, 056006 (2010).

[18] Y. M. Wang, Y. Li, and C. D. Lü, Rare decays of $\Lambda_b \to \Lambda + \gamma$ and $\Lambda_b \to \Lambda + \ell^+ \ell^-$ in the light-cone sum rules, Eur. Phys. J. C **59**, 861 (2009).

[19] Y. M. Wang, Y. L. Shen, and C. D. Lü, $\Lambda_b \to p, \Lambda$ transition form factors from QCD light-cone sum rules, Phys. Rev. D **80**, 074012 (2009).

[20] T. Gutsche, M. A. Ivanov, J. G. Korner, V. E. Lyubovitskij, and P. Santorelli, Rare baryon decays $\Lambda_b \to \Lambda l^+ l^- (l = e, \mu, \tau)$ and $\Lambda_b \to \Lambda \gamma$: Differential and total rates, lepton- and hadron-side forward-backward asymmetries, Phys. Rev. D **87**, 074031 (2013).

[21] L. Mott and W. Roberts, Rare dileptonic decays of Λ_b in a quark model, Int. J. Mod. Phys. A **27**, 1250016 (2012).

[22] L. Mott and W. Roberts, Lepton polarization asymmetries for FCNC decays of the Λ_b baryon, Int. J. Mod. Phys. A **30**, 1550172 (2015).

[23] L. L. Liu, X. W. Kang, Z. Y. Wang, and X. H. Guo, Rare $\Lambda_b \to \Lambda \ell^+ \ell^-$ decay in the Bethe-Salpeter equation approach, Chin. Phys. C **44**, 083107 (2020).

[24] H. Yan, Angular distribution of the rare decay $\Lambda_b \to \Lambda(\to N\pi)\ell^+\ell^-$, arXiv:1911.11568.

[25] P. Böer, T. Feldmann, and D. van Dyk, Angular analysis of the decay $\Lambda_b \to \Lambda(\to N\pi)\ell^+\ell^-$, J. High Energy Phys. 01 (2015) 155.

[26] T. Blake and M. Kreps, Angular distribution of polarised Λ_b baryons decaying to $\Lambda \ell^+ \ell^-$, J. High Energy Phys. 11 (2017) 138.

[27] T. Blake, S. Meinel, and D. van Dyk, Bayesian analysis of $b \to s \mu^+ \mu^-$ Wilson coefficients using the full angular distribution of $\Lambda_b \to \Lambda(\to p\pi^-)\mu^+\mu^-$ decays, Phys. Rev. D **101**, 035023 (2020).

[28] S. Meinel and G. Rendon, $\Lambda_b \to \Lambda^*(1520)\ell^+\ell^-$ form factors from lattice QCD, Phys. Rev. D **103**, 074505 (2021).

[29] S. Meinel and G. Rendon, $\Lambda_c \to \Lambda(1520)$ form factors from lattice QCD and improved analysis of the $\Lambda_b \to \Lambda(1520)$ and $\Lambda_b \to \Lambda_c^*(2595, 2625)$ form factors, Phys. Rev. D **105**, 054511 (2022).

[30] M. Bordone, Heavy quark expansion of $\Lambda_b \to \Lambda^*$ (1520) form factors beyond leading order, Symmetry **13**, 531 (2021).

[31] S. Descotes-Genon and M. Novoa-Brunet, Angular analysis of the rare decay $\Lambda_b \to \Lambda(1520)(\to NK)\ell^+\ell^-$, J. High Energy Phys. 06 (2019) 136; 06 (2020) 102(E).

[32] D. Das and J. Das, The $\Lambda_b \to \Lambda^*(1520)(\to N\bar{K})\ell^+\ell^-$ decay at low-recoil in HQET, J. High Energy Phys. 07 (2020) 002.

[33] G. Hiller and R. Zwicky, Endpoint relations for baryons, J. High Energy Phys. 11 (2021) 073.

[34] Y. Amhis, M. Bordone, and M. Reboud, Dispersive analysis of $\Lambda_b \to \Lambda(1520)$ local form factors, J. High Energy Phys. 02 (2023) 010.

[35] Z. P. Xing, F. Huang, and W. Wang, Angular distributions for $\Lambda_b \to \Lambda_J^*(pK^-)J/\psi$ decays, Phys. Rev. D **106**, 114041 (2022).

[36] Y. Amhis, S. Descotes-Genon, C. Marin Benito, M. Novoa-Brunet, and M. H. Schune, Prospects for new physics searches with $\Lambda_b^0 \to \Lambda(1520)\ell^+\ell^-$ decays, Eur. Phys. J. Plus **136**, 614 (2021).

[37] P. Guo, H. W. Ke, X. Q. Li, C. D. Lü, and Y. M. Wang, Diquarks and the semi-leptonic decay of Λ_b in the hyrid scheme, Phys. Rev. D **75**, 054017 (2007).

[38] J. Zhu, Z. T. Wei, and H. W. Ke, Semileptonic and nonleptonic weak decays of Λ_b^0, Phys. Rev. D **99**, 054020 (2019).

[39] Z. X. Zhao, Weak decays of heavy baryons in the light-front approach, Chin. Phys. C **42**, 093101 (2018).

[40] C. K. Chua, Color-allowed bottom baryon to charmed baryon nonleptonic decays, Phys. Rev. D **99**, 014023 (2019).

[41] C. K. Chua, Color-allowed bottom baryon to s-wave and p-wave charmed baryon nonleptonic decays, Phys. Rev. D **100**, 034025 (2019).

[42] H. W. Ke, N. Hao, and X. Q. Li, Revisiting $\Lambda_b \to \Lambda_c$ and $\Sigma_b \to \Sigma_c$ weak decays in the light-front quark model, Eur. Phys. J. C **79**, 540 (2019).

[43] H. W. Ke, Q. Q. Kang, X. H. Liu, and X. Q. Li, Weak decays of in the light-front quark model, Chin. Phys. C **45**, 113103 (2021).

[44] E. Hiyama, Y. Kino, and M. Kamimura, Gaussian expansion method for few-body systems, Prog. Part. Nucl. Phys. **51**, 223 (2003).

[45] T. Yoshida, E. Hiyama, A. Hosaka, M. Oka, and K. Sadato, Spectrum of heavy baryons in the quark model, Phys. Rev. D **92**, 114029 (2015).

[46] G. Yang, J. Ping, P. G. Ortega, and J. Segovia, Triply heavy baryons in the constituent quark model, Chin. Phys. C **44**, 023102 (2020).

[47] E. Hiyama and M. Kamimura, Study of various few-body systems using Gaussian expansion method (GEM), Front. Phys. (Beijing) **13**, 132106 (2018).

[48] G. Buchalla, A. J. Buras, and M. E. Lautenbacher, Weak decays beyond leading logarithms, Rev. Mod. Phys. **68**, 1125 (1996).

[49] B. Grinstein, R. P. Springer, and M. B. Wise, Effective Hamiltonian for weak radiative B meson decay, Phys. Lett. B **202**, 138 (1988).

[50] Q. S. Yan, C. S. Huang, W. Liao, and S. H. Zhu, Exclusive semileptonic rare decays $B \to (K, K^{*})\ell^{+}\ell^{-}$ in supersymmetric theories, Phys. Rev. D **62**, 094023 (2000).

[51] K. Azizi, S. Kartal, A. T. Olgun, and Z. Tavukoglu, Comparative analysis of the semileptonic $\Lambda_b \to \Lambda\ell^{+}\ell^{-}$ transition in SM and different SUSY scenarios using form factors from full QCD, J. High Energy Phys. 10 (2012) 118.

[52] W. J. Li, Y. B. Dai, and C. S. Huang, Exclusive semileptonic rare decays $B \to K^{(*)}\ell^{+}\ell^{-}$ in a SUSY SO(10) GUT, Eur. Phys. J. C **40**, 565 (2005).

[53] A. Ahmed, I. Ahmed, M. A. Paracha, M. Junaid, A. Rehman, and M. J. Aslam, Comparative Study of $B_c \to D_s^{*}\ell^{+}\ell^{-}$ Decays in Standard Model and Supersymmetric Models, arXiv:1108.1058.

[54] A. Ali, G. F. Giudice, and T. Mannel, Towards a model independent analysis of rare B decays, Z. Phys. C **67**, 417 (1995).

[55] A. J. Buras and M. Munz, Effective Hamiltonian for $B \to X_s e^{+}e^{-}$ beyond leading logarithms in the NDR and HV schemes, Phys. Rev. D **52**, 186 (1995).

[56] A. Khodjamirian, T. Mannel, A. A. Pivovarov, and Y. M. Wang, Charm-loop effect in $B \to K^{(*)}\ell^{+}\ell^{-}$ and $B \to K^{*}\gamma$, J. High Energy Phys. 09 (2010) 089.

[57] A. Khodjamirian, T. Mannel, and Y. M. Wang, $B \to K\ell^{+}\ell^{-}$ decay at large hadronic recoil, J. High Energy Phys. 02 (2013) 010.

[58] P. A. Zyla *et al.* (Particle Data Group), Review of particle physics, Prog. Theor. Exp. Phys. **2020**, 083C01 (2020).

[59] A. K. Leibovich and I. W. Stewart, Semileptonic Λ_b decay to excited Λ_c baryons at order $\Lambda_{\rm QCD}/m_Q$, Phys. Rev. D **57**, 5620 (1998).

[60] T. Feldmann and M. W. Y. Yip, Form factors for $\Lambda_b \to \Lambda$ transitions in the soft-collinear effective theory, Phys. Rev. D **85**, 014035 (2012); **86**, 079901(E) (2012).

[61] M. Pervin, W. Roberts, and S. Capstick, Semileptonic decays of heavy lambda baryons in a quark model, Phys. Rev. C **72**, 035201 (2005).

[62] C. Y. Cheung, W. M. Zhang, and G. L. Lin, Light front heavy quark effective theory and heavy meson bound states, Phys. Rev. D **52**, 2915 (1995).

[63] H. Y. Cheng, C. Y. Cheung, and C. W. Hwang, Mesonic form-factors and the Isgur-Wise function on the light front, Phys. Rev. D **55**, 1559 (1997).

[64] C. Q. Geng, C. C. Lih, and W. M. Zhang, Radiative leptonic B decays in the light front model, Phys. Rev. D **57**, 5697 (1998).

[65] H. Y. Cheng, C. K. Chua, and C. W. Hwang, Light front approach for heavy pentaquark transitions, Phys. Rev. D **70**, 034007 (2004).

[66] C. Q. Geng, C. W. Liu, and T. H. Tsai, Semileptonic weak decays of antitriplet charmed baryons in the light-front formalism, Phys. Rev. D **103**, 054018 (2021).

[67] C. Q. Geng, C. W. Liu, Z. Y. Wei, and J. Zhang, Weak radiative decays of antitriplet bottomed baryons in light-front quark model, Phys. Rev. D **105**, 073007 (2022).

[68] J. G. Korner, M. Kramer, and D. Pirjol, Heavy baryons, Prog. Part. Nucl. Phys. **33**, 787 (1994).

[69] F. Hussain, J. G. Korner, J. Landgraf, and S. Tawfiq, $SU(2N_f) \otimes O(3)$ light diquark symmetry and current induced heavy baryon transition form-factors, Z. Phys. C **69**, 655 (1996).

[70] S. Tawfiq, P. J. O'Donnell, and J. G. Korner, Charmed baryon strong coupling constants in a light front quark model, Phys. Rev. D **58**, 054010 (1998).

[71] W. Wang and Z. P. Xing, Weak decays of triply heavy baryons in light front approach, Phys. Lett. B **834**, 137402 (2022).

[72] Z. X. Zhao, Weak decays of triply heavy baryons: The $3/2 \to 1/2$ case, arXiv:2204.00759.

[73] Y. S. Li, X. Liu, and F. S. Yu, Revisiting semileptonic decays of $\Lambda_{b(c)}$ supported by baryon spectroscopy, Phys. Rev. D **104**, 013005 (2021).

[74] Y. S. Li and X. Liu, Restudy of the color-allowed two-body nonleptonic decays of bottom baryons Ξ_b and Ω_b supported by hadron spectroscopy, Phys. Rev. D **105**, 013003 (2022).

[75] S. Capstick and N. Isgur, Baryons in a relativized quark model with chromodynamics, AIP Conf. Proc. **132**, 267 (1985).

[76] S. Godfrey and N. Isgur, Mesons in a relativized quark model with chromodynamics, Phys. Rev. D **32**, 189 (1985).

[77] S. Q. Luo, L. S. Geng, and X. Liu, Double-charm hepta-quark states composed of two charmed mesons and one nucleon, Phys. Rev. D **106**, 014017 (2022).

[78] R. Aaij *et al.* (LHCb Collaboration), Observation of Two New Excited Ξ_b^0 States Decaying to $\Lambda_b^0 K^{-}\pi^{+}$, Phys. Rev. Lett. **128**, 162001 (2022).

[79] C. G. Boyd, B. Grinstein, and R. F. Lebed, Model independent extraction of $|V_{cb}|$ using dispersion relations, Phys. Lett. B **353**, 306 (1995).

[80] C. Bourrely, I. Caprini, and L. Lellouch, Model-independent description of $B \to \pi\ell\nu$ decays and a determination of $|V_{ub}|$, Phys. Rev. D **79**, 013008 (2009); **82**, 099902(E) (2010).

[81] A. Khodjamirian, T. Mannel, N. Offen, and Y. M. Wang, $B \to \pi\ell\nu_l$ Width and $|V_{ub}|$ from QCD light-cone sum rules, Phys. Rev. D **83**, 094031 (2011).

[82] C. B. Lang, D. Mohler, S. Prelovsek, and R. M. Woloshyn, Predicting positive parity B_s mesons from lattice QCD, Phys. Lett. B **750**, 17 (2015).
[83] N. Isgur and M. B. Wise, Weak decays of heavy mesons in the static quark approximation, Phys. Lett. B **232**, 113 (1989).
[84] N. Isgur and M. B. Wise, Weak transition form-factors between heavy mesons, Phys. Lett. B **237**, 527 (1990).
[85] N. Isgur and M. B. Wise, Heavy baryon weak form-factors, Nucl. Phys. **B348**, 276 (1991).
[86] T. Mannel, W. Roberts, and Z. Ryzak, Baryons in the heavy quark effective theory, Nucl. Phys. **B355**, 38 (1991).
[87] T. Mannel and Y. M. Wang, Heavy-to-light baryonic form factors at large recoil, J. High Energy Phys. 12 (2011) 067.
[88] W. Wang, Factorization of heavy-to-light baryonic transitions in SCET, Phys. Lett. B **708**, 119 (2012).
[89] R. Aaij *et al.* (LHCb Collaboration), Test of lepton universality with $\Lambda_b^0 \to pK^-\ell^+\ell^-$ decays, J. High Energy Phys. 05 (2020) 040.